JAERI-M
6102

THE FIRST RESULTS ON JFT-2a

April 1975

Y. Shimomura, T. Nagashima, A. Kitsunezaki,
H. Maeda, H. Ohtsuka, M. Nagami, T. Tokutake,
T. Ohga, T. Arai, A. Funahashi, T. Matoba
S. Kasai, T. Shoji, T. Kawakami, M. Yoshikawa
and S. Mori

日本原子力研究所
Japan Atomic Energy Research Institute

この報告書は，日本原子力研究所がJAERI-Mレポートとして，不定期に刊行している研究報告書です．入手，複製などのお問合わせは，日本原子力研究所技術情報部（茨城県那珂郡東海村）あて，お申しこしください．

JAERI-M reports, issued irregularly, describe the results of research works carried out in JAERI. Inquiries about the availability of reports and their reproduction should be addressed to Division of Technical Information, Japan Atomic Energy Research Institute, Tokai-mura, Naka-gun, Ibaraki-ken, Japan.

JAERI-M 6102

The First Results on JFT-2a

Yasuo SHIMOMURA, Takashi NAGASHIMA, Akio KITSUNEZAKI,
Hikosuke MAEDA, Hideo OHTSUKA, Masayuki NAGAMI, Toshikuni TOKUTAKE,
Katsuto ANNO, Tokumichi OHGA, Takashi ARAI, Akimasa FUNAHASHI,
Tohru MATOBA, Satoshi KASAI, Teruaki SHOJI, Tomohide KAWAKAMI,
Masaji YOSHIKAWA, Shigeru MORI

Thermonuclear Fusion Laboratory, Tokai, JAERI

(Received March 19, 1975)

JFT-2a (DIVA) is a Tokamak device with teardrop-like cross section capable of operating with an axisymmetric divertor. The research objectives of the device are to study plasma confined in teardrop-like magnetic surface configurations with and without a separatrix magnetic surface, and to investigate the characteristics of an axisymmetric magnetic limiter and/or divertor. Preliminary measurements indicate that a positionally-stable plasma enclosed in a separatrix magnetic surface is produced. The plasma extending towards the divertor hoop near the separatrix magnetic surface has a density an order of magnitude lower than that of confined plasma. In the gross behavior of the plasma, there are no significant differences whether or not the plasma is enclosed in a separatrix magnetic surface and no adverse effects of the separatrix magnetic surface on the plasma confinement are observed.

JAERI － M 6102

JFT －2 a初期実験結果

日本原子力研究所東海研究所核融合研究室
下村安夫，永島　孝，狐崎晶雄，前田彦祐，大塚英男，永見正幸，
徳竹利国，安納勝人，大賀徳道，新井　貴，船橋昭昌，的場　徹，
河西　敏，荘司昭朗，河上知秀，吉川允二，森　　茂

（1975 年 3 月 19 日受理）

JFT－2 a （DIVA）は軸対称ダイバータを設えることができる涙滴形断面トカマック装置である。本装置における研究の目的は，セパラトリックスのある場合とない場合の涙滴形断面プラズマの閉じ込めの性質を明らかにすることと，磁気リミッターあるいはダイバータの特性を研究することである。初期実験結果で以下のことが明らかとなった。セパラトリックスにかこまれた安定なプラズマを得ることができた。セパラトリックス近くの磁気面にそってダイバータ・フープ近くにプラズマが拡がってくる。このプラズマ密度は閉じ込められたプラズマの密度の約十分の 1 である。全体的なプラズマの様子はセパラトリックスがあってもなくてもあまりかわらず，セパラトリックスがプラズマの閉じ込めに悪い影響を及ぼしていないことが明らかになった。

CONTENTS

1. Introduction

JFT-2a (DIVA) is a Tokamak device with teardrop-like cross section capable of operating on an axisymmetric divertor[1)2)3)]. The design of the device was begun in 1972[4)] and some engineering tests were made in 1972 and 1973[5)]. The detailed engineering design and the construction of the device started in August 1973 and the device was put into operation in September 1974[6)].

The research objectives of the present experimental program on the device are described below.

(1) Plasma production and confinement in a Tokamak with a teardrop-like cross section with and without a separatrix magnetic surface.

A variety of cross-sectional shapes for tokamaks have been proposed in the past. A teardrop-like cross section has been chosen for the device because it appears to provide a more simple and stable configuration with a separatrix magnetic surface than the others.

A teardrop-like cross sectional shape can provide larger magnetic shear and well than the others of the same average aspect ratio, depending on the plasma parameters[3)]. Consequently, the current density limit required to stabilize local instability is higher than in cases of a flat current distribution, and of a parabolic distribution at low-β[7)].

A plasma equilibrium with a separatrix magnetic surface is given in a poloidally incomplete shell and a divertor hoop which can carry a current proportional to a plasma current[8)]. Magneto-hydrodynamic stability of a plasma may be provided by the shell.

The differences between the characteristics of confined plasmas with or without a separatrix magnetic surface are to be studied as well as the plasma behavior at the separatrix magnetic surface.

(2) Characteristics of a divertor or a magnetic limiter[2)]

In a large Tokamak device of an ordinal type, damage to the wall including the material limiter is serious and large impurity content is inevitable. A divertor and/or magnetic limiter offers a possibility of reducing damage and of lowering impurity content by guiding the plasma particle and heat fluxes to the burial chamber. In the burial chamber, it is possible to disperse the fluxes on a larger surface area of the neutralizer plate to reduce the heat loading and damage, and also to

capture the sputtered and back scattered particles in the burial chamber to reduce impurity contamination.

An experimental study is to be made on the operation of an axisymmetric divertor. Plasma equilibrium in the required plasma configuration, particle and energy transport on the divertor magnetic surfaces, and basic operational characteristics of the divertor are also to be studied experimentally. Investigation will be also made concerning neutral particle effects on the plasma.

To make research on these objectives, the design of the device is made under the following guide lines:

Conservative design, wherever possible

Comparison to be possible with and without a magnetic limiter and/or a divertor, and

Impurity and neutral particle release at the wall to be minimized, since the divertor plasma is likely to be "transparent" to the particle influx from the wall.

This report contains the descriptions of the device, the diagonostic methods, and the preliminary experimental results.

2. Description of JFT-2a[1)2)3)]

Basic machine parameters are shown in Table 1 and the cross-sectional and the plan view of the device are shown in Fig. 2-1, Fig. 2-2 and Fig. 2-3, respectively. Photographs of the device are also shown in Fig. 2-4 and Fig. 2-5. The detailed descriptions of the main components of the device are given below.

2.1 Shell

The copper shell enclosing the plasma is 2-3 cm in thickness and contained within a vacuum chamber as shown in Fig. 2-2 and Fig 2-5. The time constant of the penetration of vertical magnetic field into the shell is about 80 ms. A quarter sector of the shell is shown in Fig. 2-6. The toroidal opening between the two neighboring sector is 4° (3~5 cm).

The surface of the shell is ion-plated with gold of 10~20μ in thickness. Atomic compositions of the gold film is shown in Fig. 2-7. It is shown that the ion-plated gold film can provide the extremely clean wall

capture the sputtered and back scattered particles in the burial chamber to reduce impurity contamination.

An experimental study is to be made on the operation of an axisymmetric divertor. Plasma equilibrium in the required plasma configuration, particle and energy transport on the divertor magnetic surfaces, and basic operational characteristics of the divertor are also to be studied experimentally. Investigation will be also made concerning neutral particle effects on the plasma.

To make research on these objectives, the design of the device is made under the following guide lines:

Conservative design, wherever possible

Comparison to be possible with and without a magnetic limiter and/or a divertor, and

Impurity and neutral particle release at the wall to be minimized, since the divertor plasma is likely to be "transparent" to the particle influx from the wall.

This report contains the descriptions of the device, the diagonostic methods, and the preliminary experimental results.

2. Description of JFT-2a[1)2)3)]

Basic machine parameters are shown in Table 1 and the cross-sectional and the plan view of the device are shown in Fig. 2-1, Fig. 2-2 and Fig. 2-3, respectively. Photographs of the device are also shown in Fig. 2-4 and Fig. 2-5. The detailed descriptions of the main components of the device are given below.

2.1 Shell

The copper shell enclosing the plasma is 2-3 cm in thickness and contained within a vacuum chamber as shown in Fig. 2-2 and Fig 2-5. The time constant of the penetration of vertical magnetic field into the shell is about 80 ms. A quarter sector of the shell is shown in Fig. 2-6. The toroidal opening between the two neighboring sector is 4° (3~5 cm).

The surface of the shell is ion-plated with gold of 10~20μ in thickness. Atomic compositions of the gold film is shown in Fig. 2-7. It is shown that the ion-plated gold film can provide the extremely clean wall

for a plasma compared with the wall made of stainless steel (Fig. 2-8). Therefore, impurity release at the wall in this device may be much less than in a device without a gold surface. The formation and the characteristics of the gold surface were studied and reported in 1972).

Part of the shell, the movable shell, can be moved vertically in 10 sec. by electric motors set outside of the vacuum chamber as shown in Fig. 2-9. For plasma confinement with the complete shell in operation, the movable shell is at the "closed" position as shown in Fig. 2-2. The operation of the divertor or the magnetic limiter is studied by setting the movable shell at the "open" position. The movable shell can also be operated as a "shutter" for titanium vapor during the operation of titanium flushing.

The cross-sectional shape of the inner surface of the shell is expressed by the equation,

$$((R-R_0)^2 + Z^2)(1 - \varepsilon_2\cos 2\theta) - \frac{\varepsilon_3}{\bar{a}} ((R-R_0)^2 + Z^2)^{\frac{3}{2}} \cos 3\theta = \bar{a}^2$$

where R_0 = 59cm, $\bar{a}$ = 11.43cm, ε_2 = 0.27 and ε_3 = -0.17[9].

The equilibrium and localized instability of a plasma with the shell studied numerically and reported in ref. (9).

2.2 Limiter

The limiter shown in Fig. 2-10 consists of three molybdenum pieces clad in gold of 1 mm in thickness which are manually retractable. The gold surface is employed also on the limiter to lower desorption of atoms from the limiter and to prevent foreign materials from contaminating the gold-plated surface of the shell. The sputtering yield of gold by an energetic atom is several times larger than that of molybdenum and the heat characteristics of gold is not so good as those of molybdenum as shown in Table 2. The limiter is cooled to 400°K or less by water during an interval between successive discharges. In this small device, the impurity content of heavy atoms such as gold may be small.

To protect the inner surface of the shell, six small gold pieces, protection plates, of 1 mm in thickness are set at the edge of one of the sectors of the shell, extending 5 mm from the shell, as shown in Fig. 2-10.

2.3 Divertor System

The divertor system consists of a divertor hoop carrying a current

proportional to a plasma current, divertor plates made of titanium and a titanium flushing system.

The divertor hoop is a four-turn coil enclosed in a vacuum-tight stainless steel tube located inside the vacuum chamber and maintains a plasma equilibrium with a separatrix magnetic surface which is for the most part encased in the shell.

The divertor hoop consists of two semi-circular portions with two vacuum-tight connecting joints so that the device can be disassembled. The connecting joint is shown in Fig. 2-11. The major radius and minor radius of the hoop are 37 cm and 1.6 cm, respectively. A pair of divertor plates, neutralizer plates, are made of 99.9% titanium, are attached to the stainless steel tube of the hoop and intersect the separatrix magnetic surface. The hoop is cooled by air at 330 °K. Cross-sectional view of the hoop is shown in Fig. 2-12.

The stainless steel tube of 2 mm in thickness not only supports the four-turn coil made of copper but also reduces the toroidal electric field induced by a sudden change of a plasma current and inductance. The time constant of the tube is about 250 μsec.

The hoop carries a current in proportion to a plasma current and the maximum m.m.f. is 60 kAT. Power supply system is described in 2.5.

As memtioned before, a pair of divertor plates made of titanium attached to the divertor hoop to neutralize or adsorb particles from the confined plasma. The fresh titanium surface absorbs various kinds of gases including H_2, O_2, CO_2 and CO, and is chosen as the surface material near the divertor hoop in the operation of the divertor.

Titanium alloy wires for flushing are set along the torus as shown in Fig. 2-13. Titanium evaporation was studied experimentally and an optimum operation mode was determined. About 6×10^{19} titanium atoms is evaporated in an operation and an average of two atomic layers may be produced over an area of about 2.5×10^4 cm^2. A set of titanium alloy wires can be flushed 2000-3000 times.

Sticking process of neutral particles was studied by a Monte-Carlo calculation and reported in ref. (2).

2.4 Magnetic Field System

Toroidal magnetic field of 10 kG at R=60 cm is produced by 16 coils each having 26 turns. To provide a large space required for installing

diagnostics equipments and assembling the device, the coil of a simple structure. Shown in Fig. 1 and Fig. 3 have been chosen. Consequently, the uniformity of the magnetic field is not very good as can be seen in Fig. 2-14, the deviation of the field intensity in a plasma region being about 3 % and the spatial ripples of field lines are less than 1 mm.

The stray field due to current feeders and windings of the coils can be compensated for by adjusting the position of two parallel conductors of the return windings of the coils.

The current of the coils is supplied by SCR controlled rectifiers of 4700 kVA and the duration time of the current is 2 sec. The time constant of the coil is 0.68 sec and the current ripple is less than 0.1 %. The coils are cooled by water running through holllow copper conductors.

A DC vertical magnetic field of 120 G at maximum is produced by two coils and two return coils shown in Fig. 2-1. Stability factor of the vertical field for circular cross section plasmas $n = R/B_V \times dB_v/dR$ is about -0.3. The current for the vertical field coils of 40 kAT is supplied by a motor-dc generator set.

A horizontal magnetic field of 20 G at maximum is produced by two coils located near the vertical magnetic coils. The horizontal field is adjusted so as to locate the plasma on the median plane. These coils are connected to the toroidal magnetic coils in series with a variable resistor in parallel.

The repitition rate of the device is limited by that of the toroidal field coils to one shot every three minutes.

2.5 Power Supply System for Plasma and Divertor Hoop

Currents of a plasma and the divertor hoop are supplied by a capacitor bank through two current transformers which are named the main transformer and the hoop transformer (see Fig. 2-15).

The main transformer consists of an iron core of 0.3 V.sec in flux, and a primary winding T_1 of 96 turns with two taps at the 72nd and 48th turn, and a four-turn return winding T_R of the divertor hoop. The primary windings T_{D1} of the loop transformer has 150 turns with a tap at the 75th turn, and the secondary windings T_{D2} of 18 turns has two taps at 16th and 14th turn which are connected to the divertor hoop and the return winding of the divertor hoop.

The total energy of the condenser bank is 95 kJ. To supply a large

one-turn voltage and to sustain a plasma current at a constant value for several m sec, two small banks of condensers are discharged one after another. One of them consists of condensers of the working voltage of 10 kV and a capacitance of 100 μF (5kJ), and the other consists of condensers of 5 kV and 7200 μF (90kJ).

The capacitor bank is connected through a ignitor switch to the primary windings of the two transformers in series as shown in Fig. 2-15. By employing such a circuit the ratio of the hoop current and the plasma current can be kept constant during a discharge except in a case when the plasma resistivity remains extremely high during the discharge. The ratio is adjustable from 0.2 to 0.9 with taps described above.

The stray vertical field due to the magnetization of an iron core by a secondary current (plasma current) was measured in the model iron transformer of the JFT-2a device. The result is extended to the case of the JFT-2a device by scaling law in electromagnetism. It is reduced to be about 3.7G/(1kA of plasma current) at R=60 cm and homogeneous along the torus within 2.5%.

2.6 Vacuum System

The vacuum chamber is made of stainless steel and consists of two toroidal sections which are electrically insulated between each other by teflon sheets of 12 mm in thickness. The net volume of the vacuum chamber is 430 ℓ and the volume surrounded by the shell is 170 ℓ. About 120 ports are attached to the chamber for measurements of plasmas, setting of the shell and so on. Viton packings are employed to seal the vacuum chamber. Many parts of the device are contained in the chamber and the main surfaces exposed to the vacuum are

stainless steel (5.5×10^4 cm^2),
oxygen-free copper ion-plated with gold (4×10^4 cm),
Viton (80 cm^2),
teflon (5×10^3 cm^2) and
alumina (5.4×10^3 cm^2).

The main pumping circuit consists of one primary rotary pump and two parallel turbo-molecular pumps. The measured pumping speed is about 560 l/sec at a pressure of 5×10^{-6} Torr (N_2). The vacuum chamber is bakable at a temperature of 110 °C. The minimum pressure of the chamber obtained in the past is 3×10^{-8} Torr and the main components of the residual gas are N_2 and O_2.

The average thickness of the stainless steel of the chamber is 8 mm and the time constant of the penetration of toroidal magnetic field is about 1.1 msec.

2.7 Gas Supply System

Plasmas are produced by two gas supply methods. One is the continuous gas supply and the other is the pulsed gas admission into the shell just before the discharges. Continuous admission of hydrogen gas at a rate of 0.1 Torr·l/sec into the vacuum chamber results in 2×10^{-4} Torr of filling pressure. Pulsed gas admission of about 200 μsec time duration is achieved by four fast acting gas valves. The valves each with a plenum volume of 0.2 cm^2 at a filling pressure when the admitted gas spreads within the shell. The purity of the supplied hydrogen gas is higher than 99.9 %. The power to actuate these fast acting gas valves is supplied by a capacitor bank of 40 μF and 3 kV. The coils of the valves are connected in series and the total inductance of this circuit is about 5 μH.

Four fast acting valves are employed for the quick filling of the device to minimize the absorption of gas to the wall surface and to keep the refreshed surfaces covered with titanium as clean as possible before the discharge takes place. The setting positions of these valves are shown in Fig. 2.3.

2.8 Pre-ionization System

For the initial ionization of the gas in the device microwave discharge at the electron cyclotron resonance frequency and breakdown due to the energetic electrons emitted from an electron gun are available.

The electron cyclotron frequency is found to be 28 GHz, where the toroidal magnetic field is 10 kG. For heating we use a travelling tube operating at 28 HGz and with the maximum power 1 kW and the microwave pulse length 2 msec. The energy is fed into the chamber by means of a rectangular waveguide with a little attenuation.

Electrons emitted from the filament are accelerated by the biasing electric fields applied to the filament and drifted into the minor axis of the torus due to a toroidal magnetic field. For the filament we use 0.5-mm-diam. tungsten wire with an effective emitting length of 2 cm located along the toroidal magnetic field. The heating time of the filament is from 2 to 90 sec. The voltage and the width of the accelerating pulse are 0.1-3 keV and 0.1-2 msec, respectively. The operation of the electron

gun is determined from the contamination rate of the gold coated shells by the evaporated tungsten atoms from the filament.

The electron density of the preionized plasmas by these two methods is expected to be 10^9-10^{10} cm^{-3} in a hydrogen discharge.

Table 2.1 Basic Parameters of JFT-2a

Toroidal Magnetic Field		1.0 T
Vertical Magnetic Field		1.2×10^{-2}T
Magnetic Flux of Iron Core		0.3 Vs
Shell	Major Radius	600 mm
	Inner Minor Radius	105×140 mm
	Thickness	20 mm
Maximum Divertor Hoop Current		60 kAT

Table 2.2 Heat characteristics of metals

	C $(\frac{\text{Joule}}{\text{g.deg}})$	ρ (g/cm^3)	λ (W/cm deg)	Melting point T_m °C	$\sqrt{\rho c\lambda}\,(T_m - T_o)$		
					T_o=0°C	T_o=200°C	T_o=800°C
W	0.126	20	1.7	3400	7000	6600	5400
Mo	0.252	10	1.4	2600	4900	4500	3700
Ta	0.126	17	0.4	3000	2800	2600	2000
C	0.42	2	2.5	3800	5500	5200	4300
Au	0.126	20	3.1	1060	3000	2400	730
Cu	0.42	9	4	980	3800	3000	700
SUS	0.42	8	0.14	1500	1000	710	380

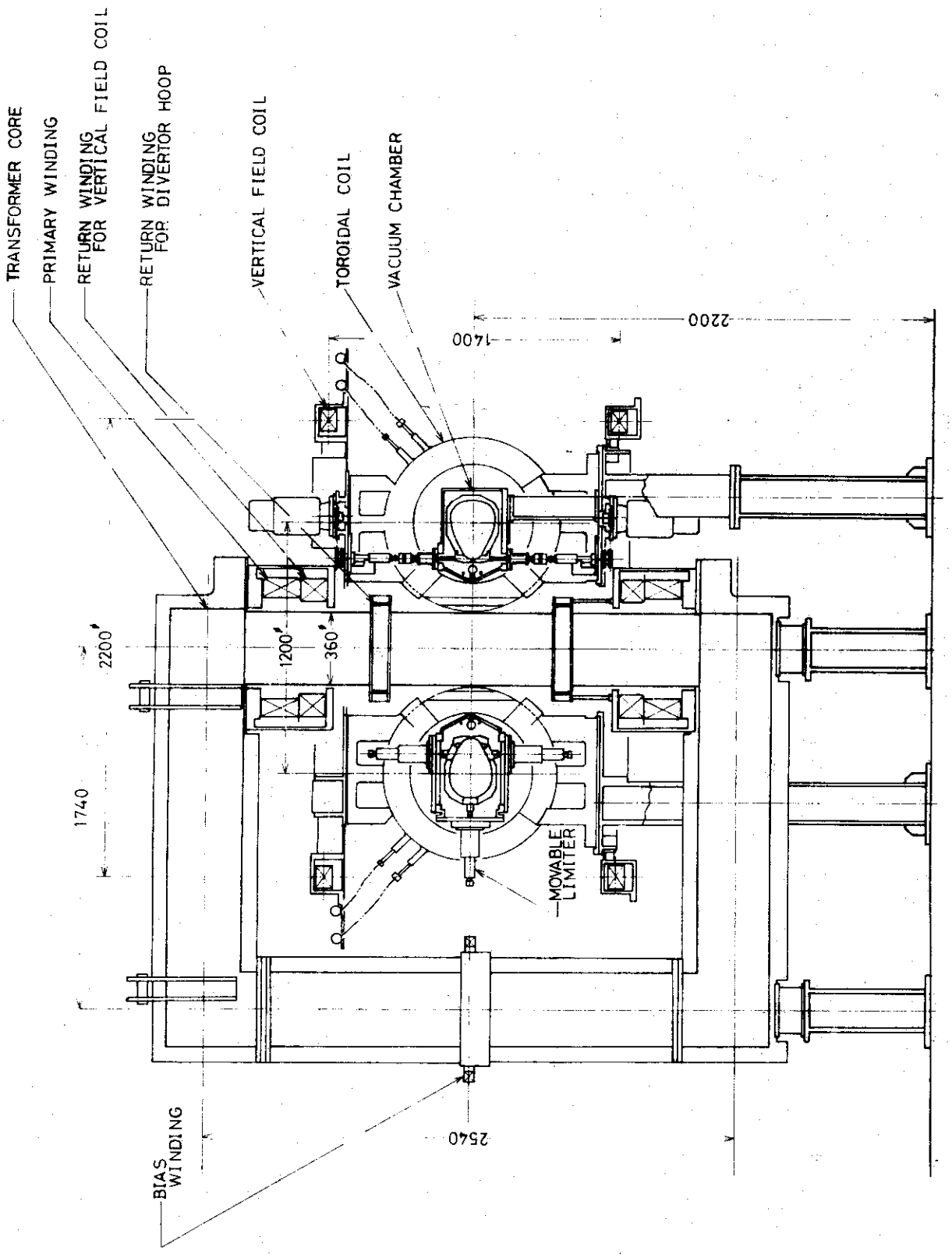

Fig. 2-1 Cross section of JFT-2a

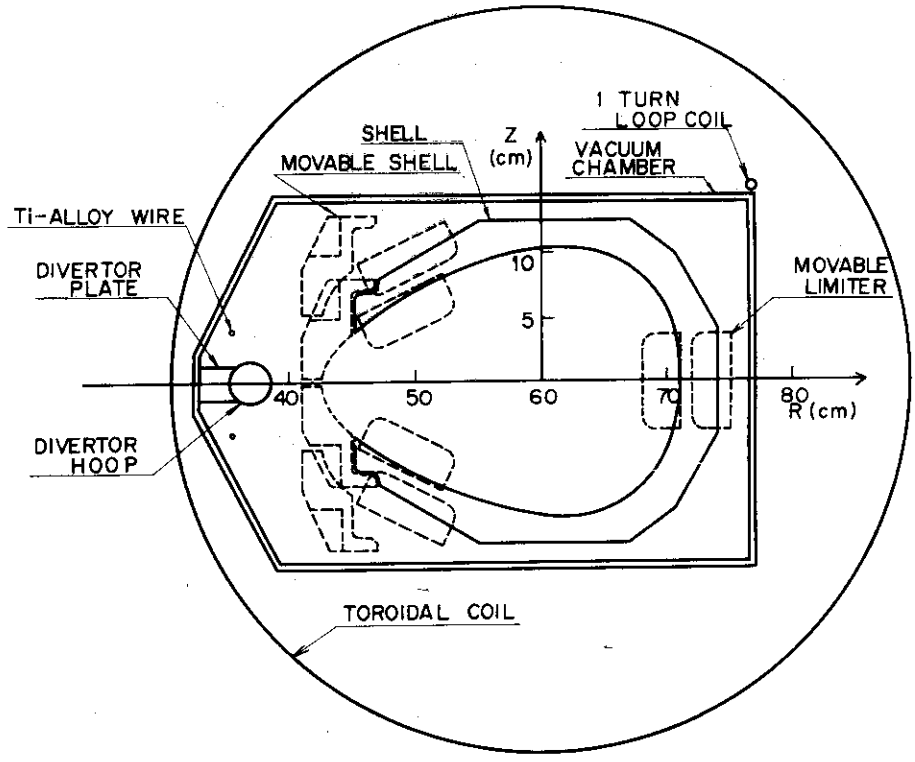

Fig. 2-2 Cross section of vacuum chamber

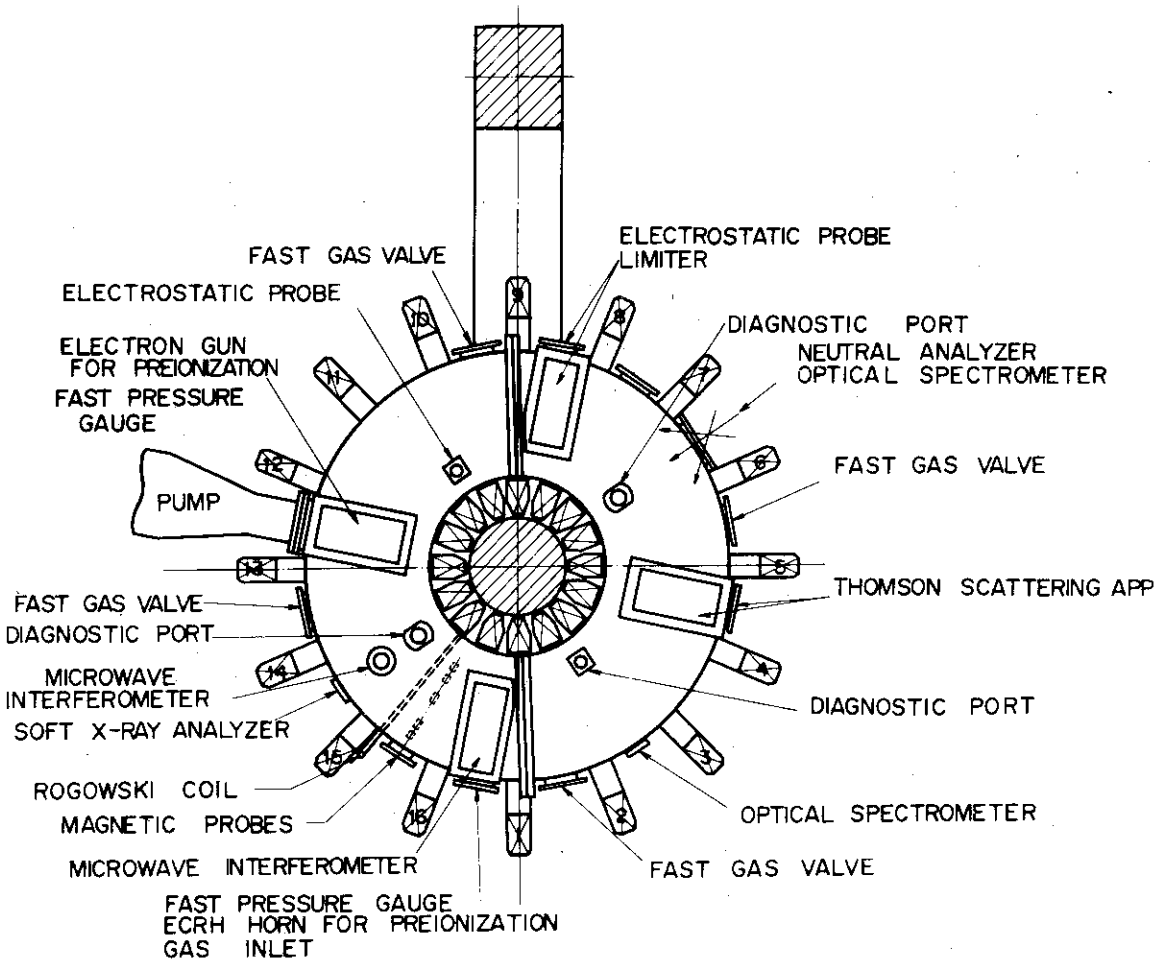

Fig. 2-3 Plan view of the device

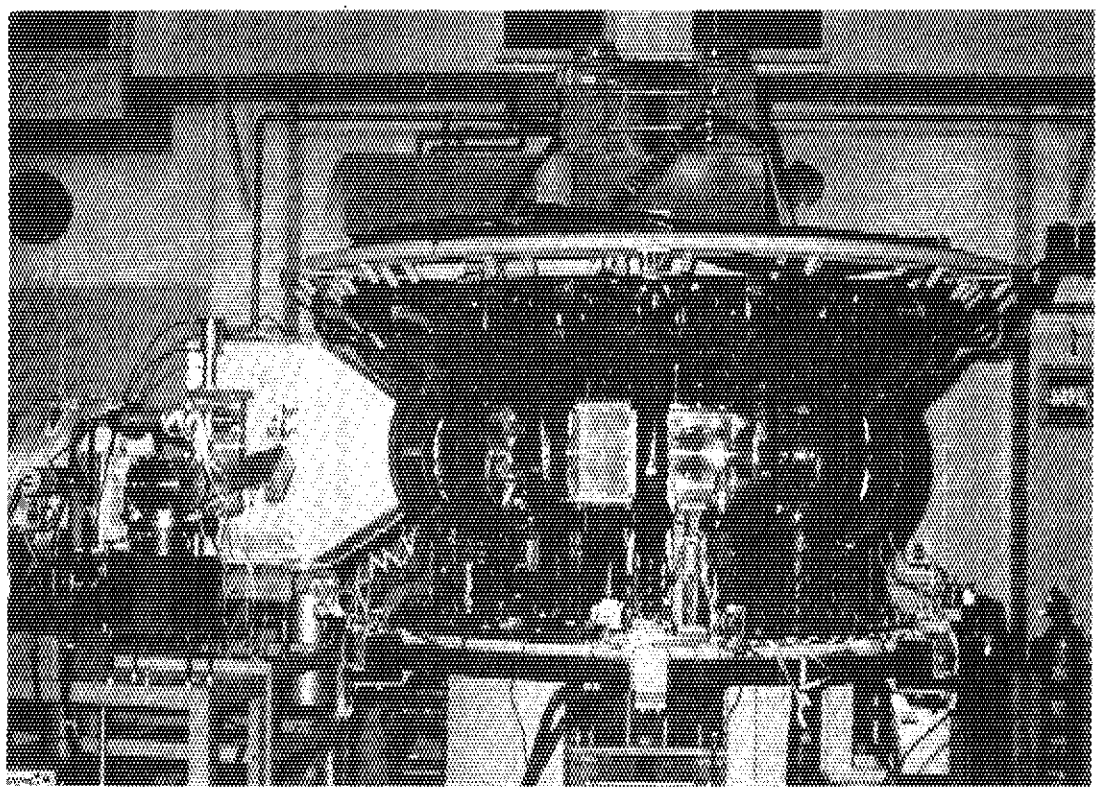

Fig. 2-4 Photograph of the device

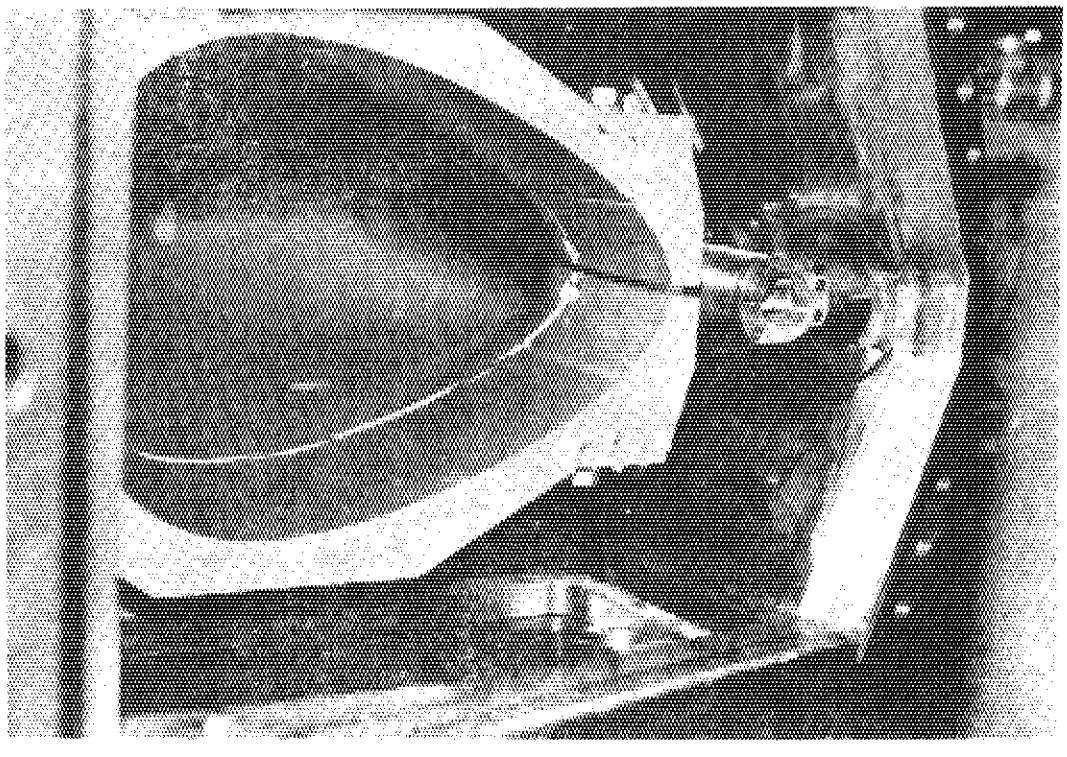

Fig. 2-5 Photograph of joining part of vacuum chamber

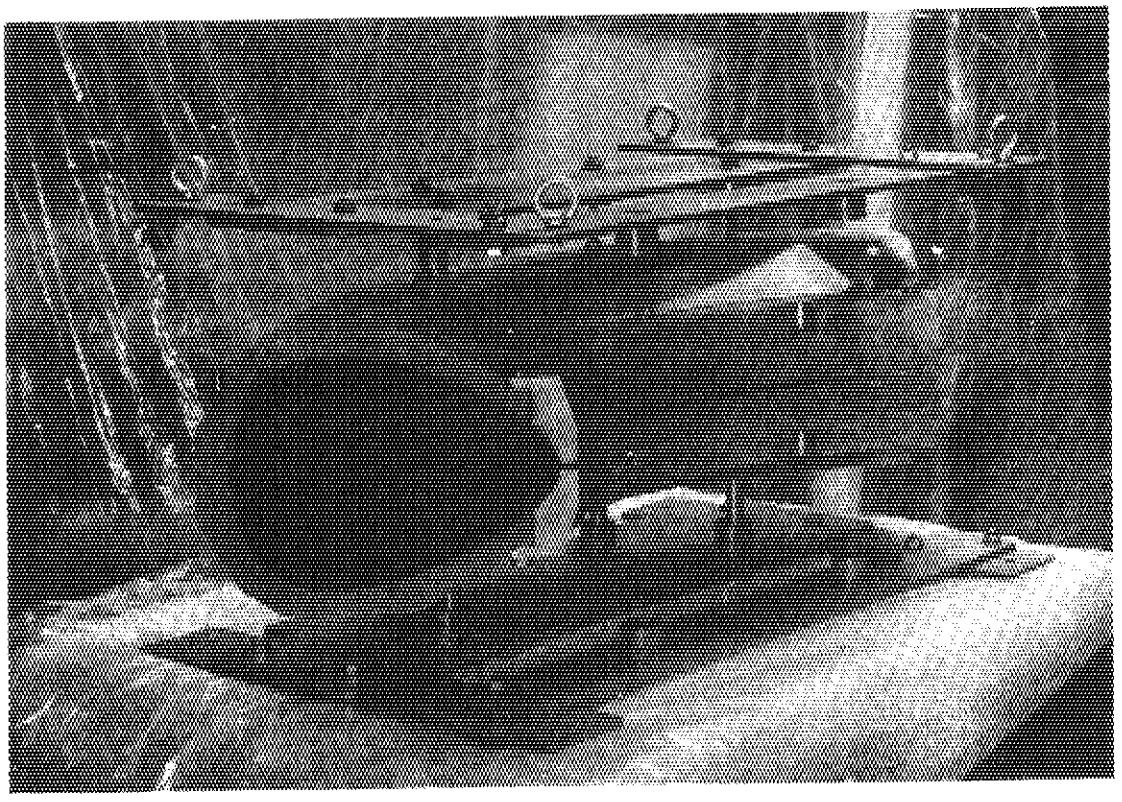

Fig. 2-6 Photograph of shell

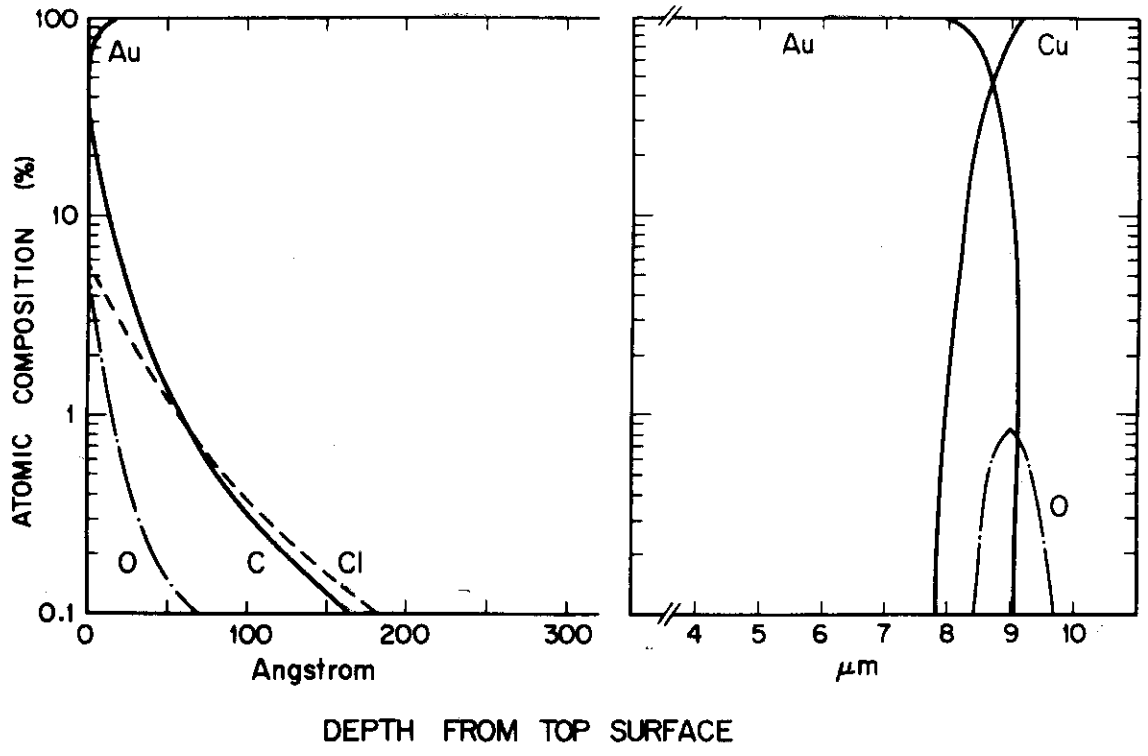

Fig. 2-7 Depth distribution of atomic composition of ion-plated on copper obtained by AES

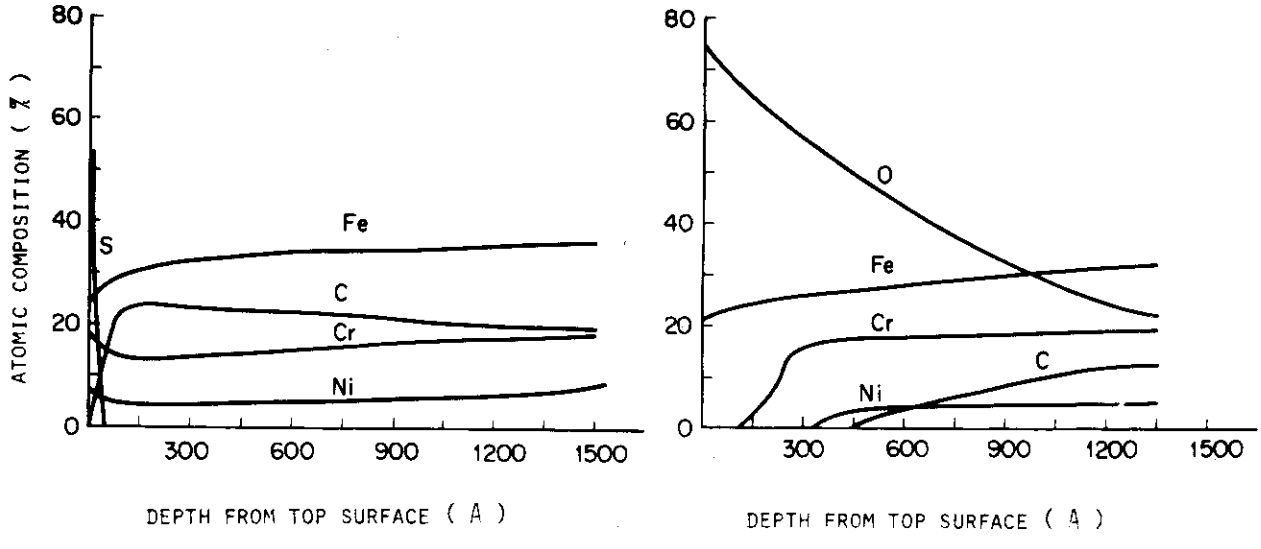

Fig. 2-8 Depth distribution of atomic composition of stainless-steel obtained by AES
(a): after being baked at 1000°C in vacuum
(b): after being baked at 40°C in atmosphere

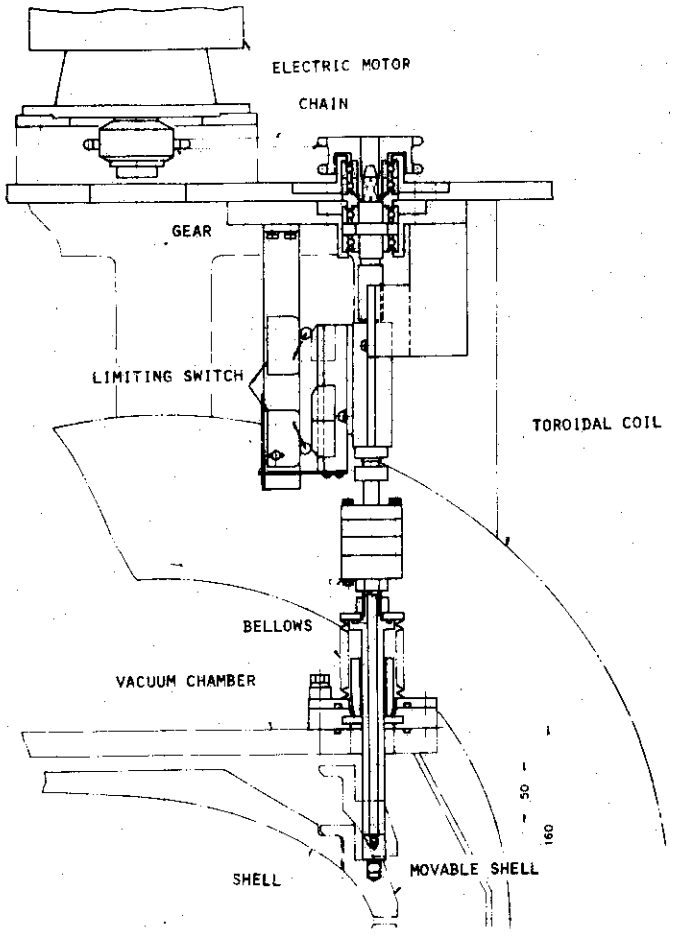

Fig. 2-9 Movable shell and its driving system

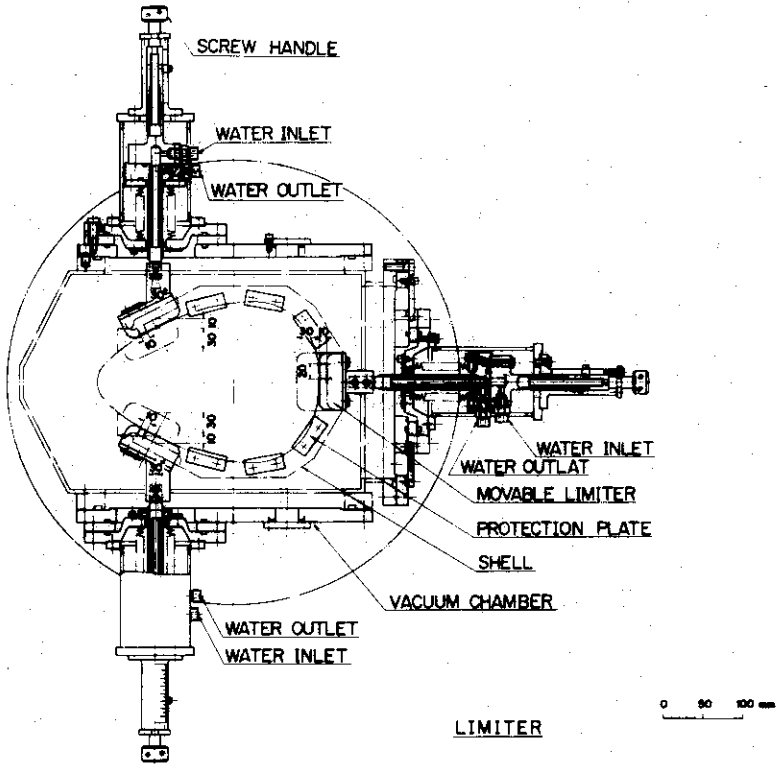

Fig. 2-10 Limiter

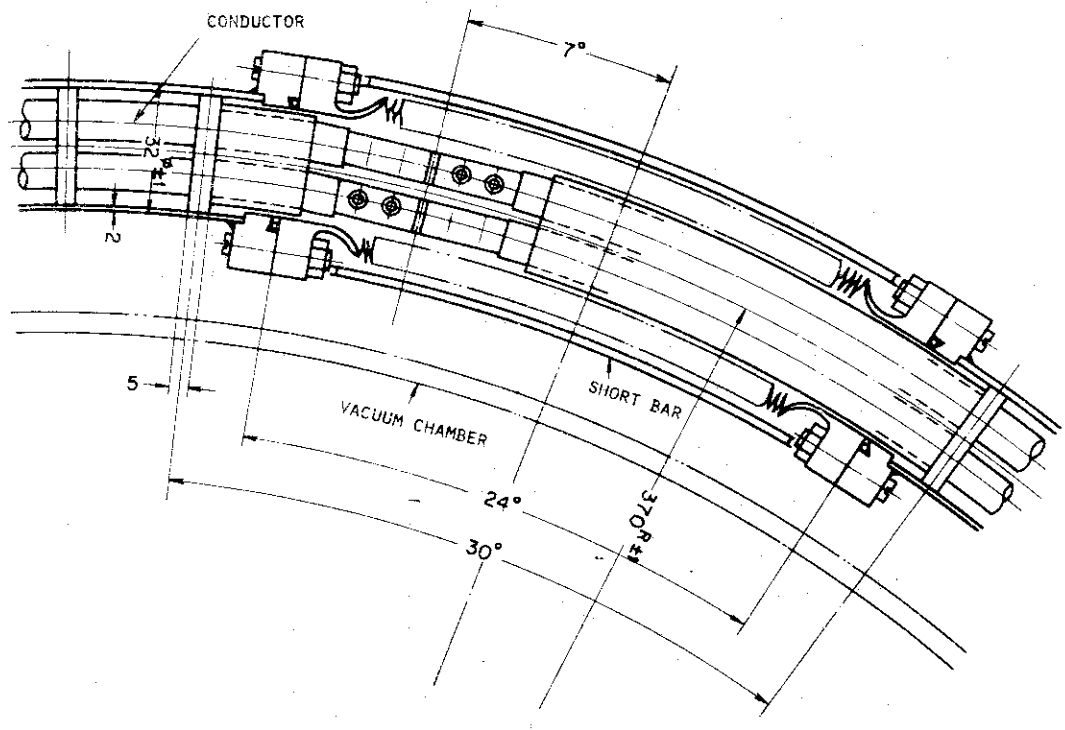

Fig. 2-11 Connecting joint of divertor hoop

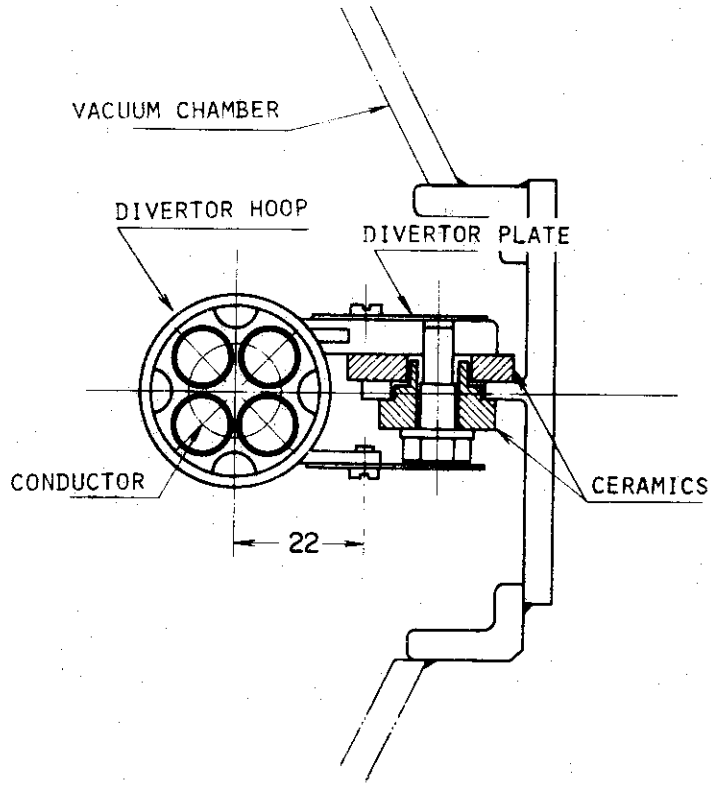

Fig. 2-12 Cross section of divertor hoop

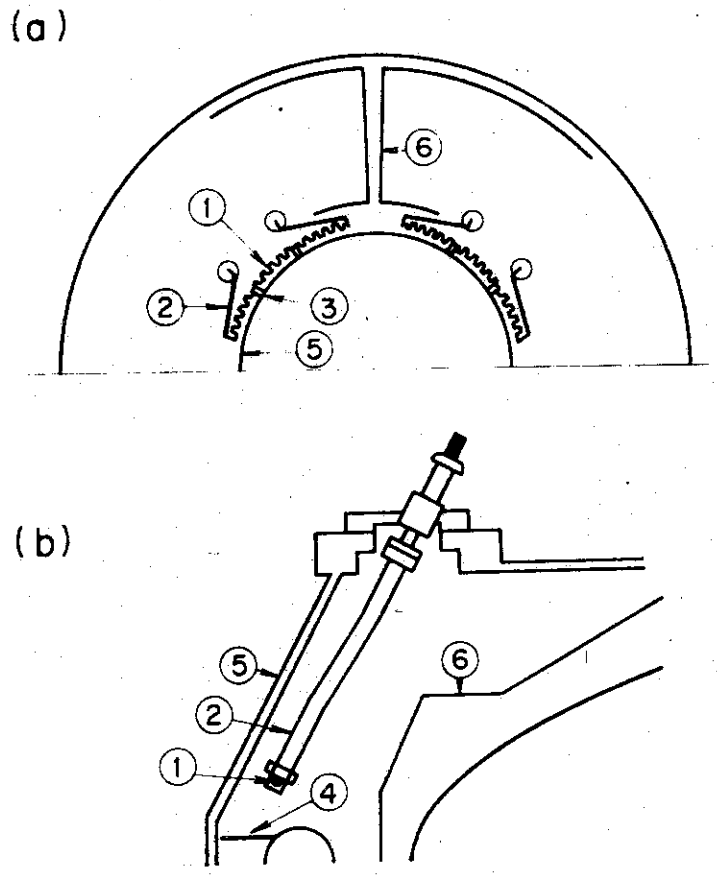

Fig. 2-13 Titanium alloy wire for flushing

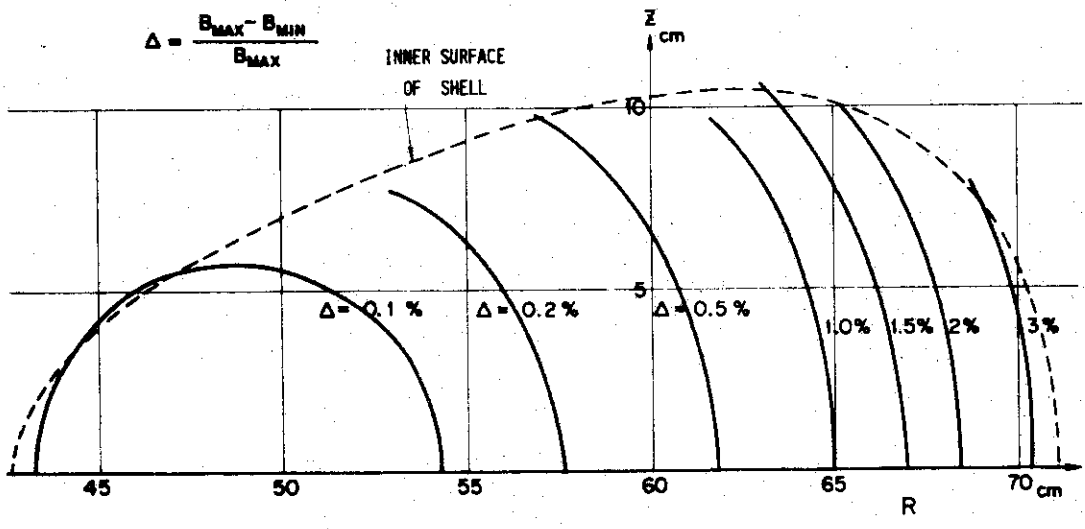

Fig. 2-14 Deviation of toroidal field intensity

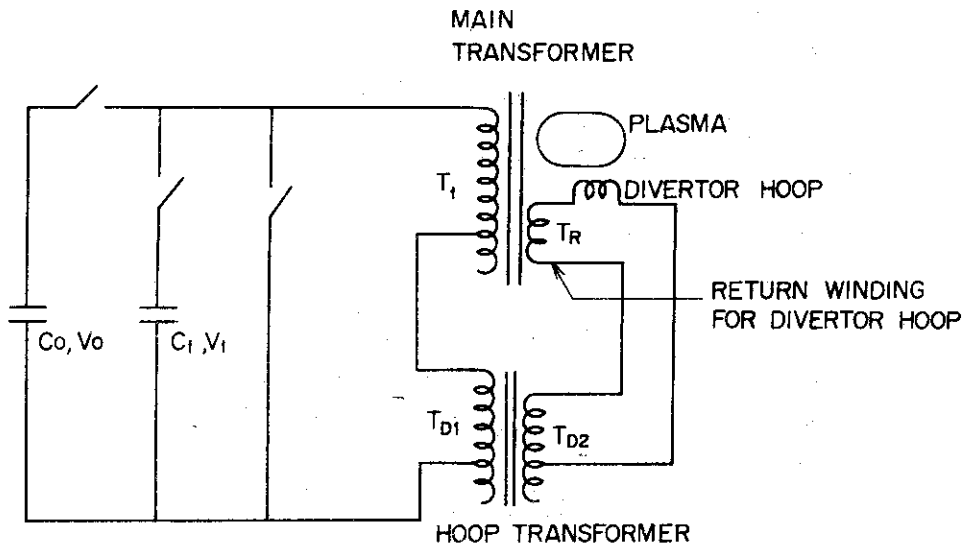

$C_0 \leq 200\ \mu F$ $\quad T_1$: 96,72 and 48 Turns

$V_0 \leq 10$ KV $\quad T_{D1}$: 150 and 100 Turns

$C_1 \leq 7200\ \mu F$ $\quad T_{D2}$: 18 , 16 and 14 Turns

$V_1 \leq 5$ KV

Fig. 2-15 Circuit diagram of power supply for plasma and divertor hoop

3. Diagnostics

Essential plasma parameters characterizing a tokamak discharge are mostly measured by those methods which have already applied to JFT-2. These standard methods[10] are summarized below.

Plasma parameter	Measuring methods
Plasma current	Rogowski coil measurement
One-turn voltage	One-turn loop measurement
Poloidal field	Magnetic probe measurement
Electron temperature	Laser scattering
	X-ray analysis
Ion temperature	Neutral particle analysis
	Doppler broadening of impurity lines
Electron density	Three-channel 4 mm microwave interferometer
Hydrogen atom density	Spectroscopy
	Neutral particle energy analysis
Impurity	Spectroscopy in visible and vacuum UV lines

The investigation of the magnetic limiter and/or divertor calls for further methods which can measure plasma parameters at the boundary of a main plasma column and near the divertor hoop. Local plasma parameters such as electron temperature and density, electric field and fluctuations are measured with electrostatic probes. The neutral particle density is determined by fast ionization gauges. The energy and the particle flux to the divertor will be estimated by thermocouple measurements and electron density distribution measurement, respectively. Spectroscopic methods will be employed to measure the local impurity content.

The positions of observation ports are shown in Figs. 2-2 and 2-3.

4. Experimental Results

The experimental results described in this section is obtained under the following conditions. The toroidal field is fixed at 1 T and no vertical field is applied. The horizontal field is adjusted so to locate a plasma on the median plane with the exception of early discharges. The divertor hoop current is varied up to 90 % of a plasma current. The movable shell is at open position, the limiters extend 1 cm from the shell, and no titanium is flushed. The base pressure is $(0.3 - 1.5) \times 10^{-7}$ Torr. Hydrogen gas of $(0.4 - 2) \times 10^{-4}$ Torr in pressure is introduced through a variable leak valve or four fast acting valves.

More than 10,000 discharges have been performed where preliminary measurements were made. The plasma current Ip the one turn voltage V_L, the divertor hoop current I_D, the vertical plasma displacement Δv, the poloidal field distribution and its fluctuations along the inner surface of the shell, the electron density from a single channel zebra-stripe 4 mm microwave interferometer and electrostatic probes, the neutral particle density of the outside of the shell, the visible and VUV radiations and the hard X-ray radiation are measured. The other measurements including laser scattering, neutral particle energy analysis, soft X-ray analysis, multi-channel microwave interferometory and thermocouple measurements are under preparation.

4.1 Plasma Behavior during the Discharge Cleaning

Early discharges are macroscopically unstable and/or are characterized by runaway electrons presumably because of the uncleanliness of the shell and limiter surfaces which had been treated with insufficient care and of the horizontal error fields of about 10^{-3} T due to the toroidal coil misalignment. The error field was compensated by the horizontal coils so to locate the plasma on the median plane. After several hundreds of discharges, the surfaces of the limiter and the shell near the limiter were found locally contaminated in stripes by black material. The black increased as the shot number increased up to about two thousand and then decreased. After about four thousand discharges, this black material became unrecognizable, and stable and reproducible discharges were obtained.

Before starting daily measurements, it is customarily needed to perform 30-60 discharges of 20 kA current pulses of 20-40 ms duration for 1 ~ 2 hours to obtain stable and reproducible discharges. Figure 4-1 shows

oscillograms of these preparatory discharges. It is seen that large negative spikes appear intermittently in the loop voltage in the first discharge of the day accompanied by the density and the H_α line fluctuations which decrease with the increasing the number of discharges. It can be seen that the second peak of the electron line density at R = 63 cm decreases with the shot number. The height of the second peak approaches constant value after 30 - 50 discharges as shown in Fig. 4-2.

After venting the vacuum vessel for a day or less, it is necessary to perform about 200 shots of such discharges to obtain stable and reproducible discharges.

The variation of the characteristics of the early discharges after opening the vacuum vessel to the atmosphere for a month or so is shown in Figs. 4-3 and 4-4. The pressure outside of the shell increases above the filling pressure and the plasma resistivity is extremely high during the first 20 - 30 discharges. After more shots are fired, we obtain those discharges in which the pressure outside of the shell decreases greatly during a discharge, and find that the resistivity and negative spikes are reduced. About one thousand discharges are required to obtain such stable and reproducible discharges.

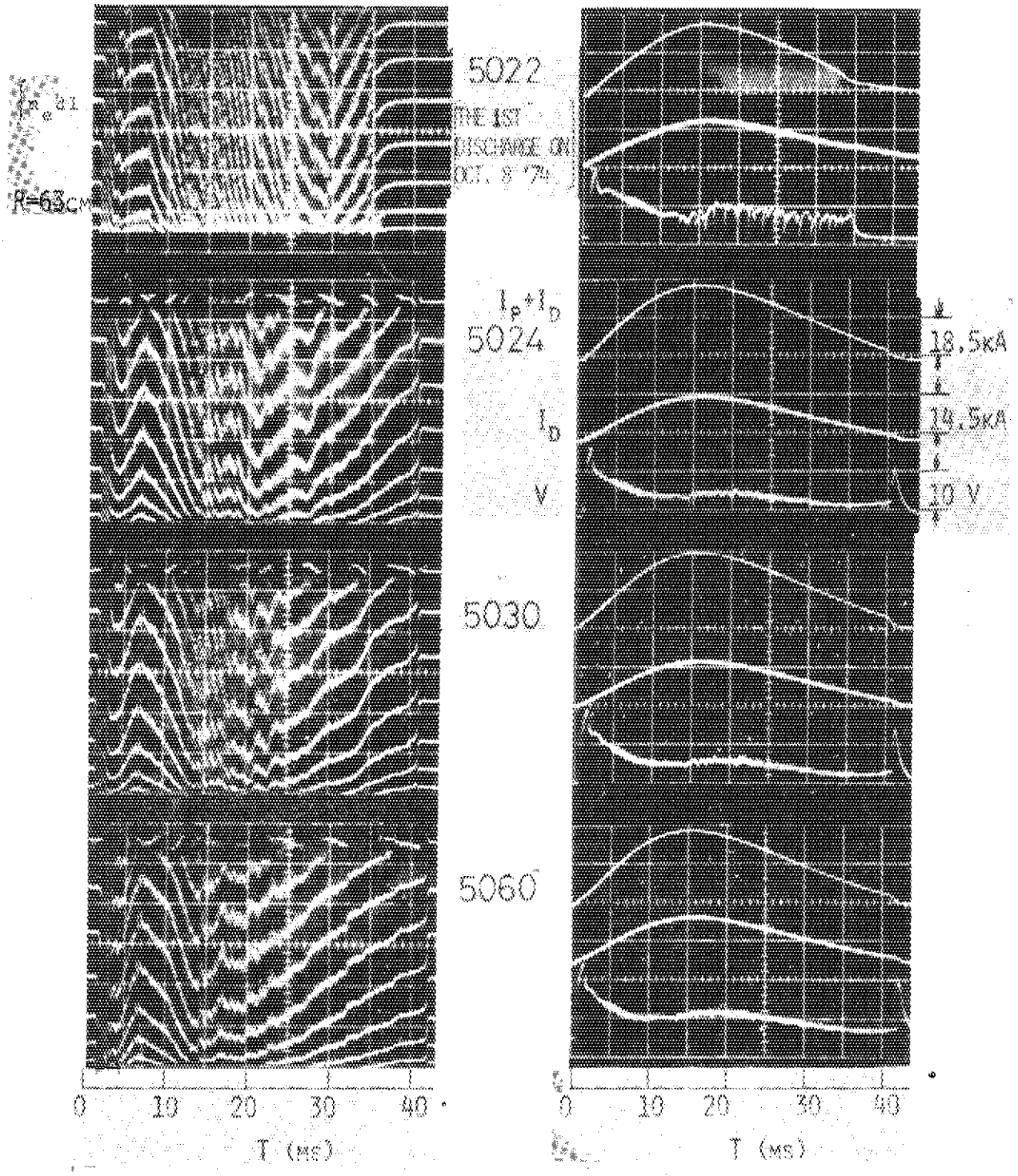

Fig. 4-1 Oscillograms of sum of plasma current I_p and divertor hoop current I_D, I_D, loop voltage V, electron line density, and light intensity of H_α line. The operation condition is I_D/I_p = 0.9, B_V = 0 and the continuous filling pressure = ~1.4×10^{-4} Torr.

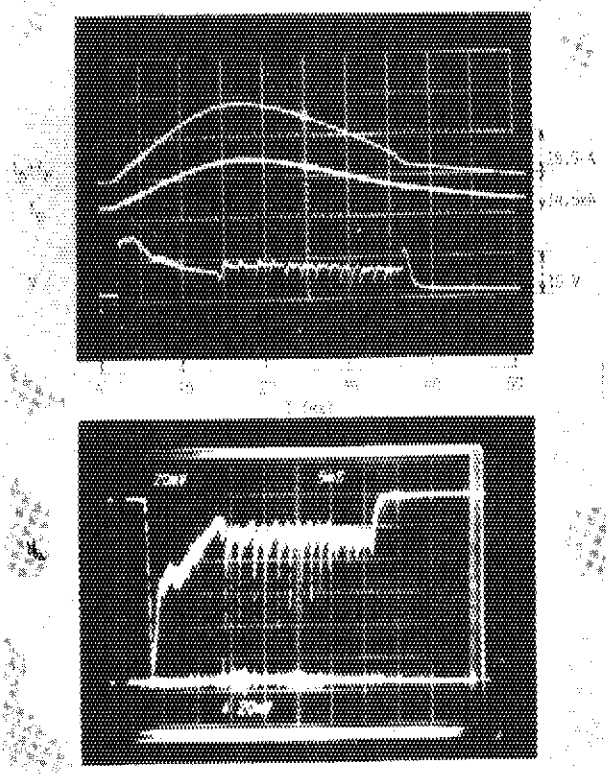

Fig. 4.1.b

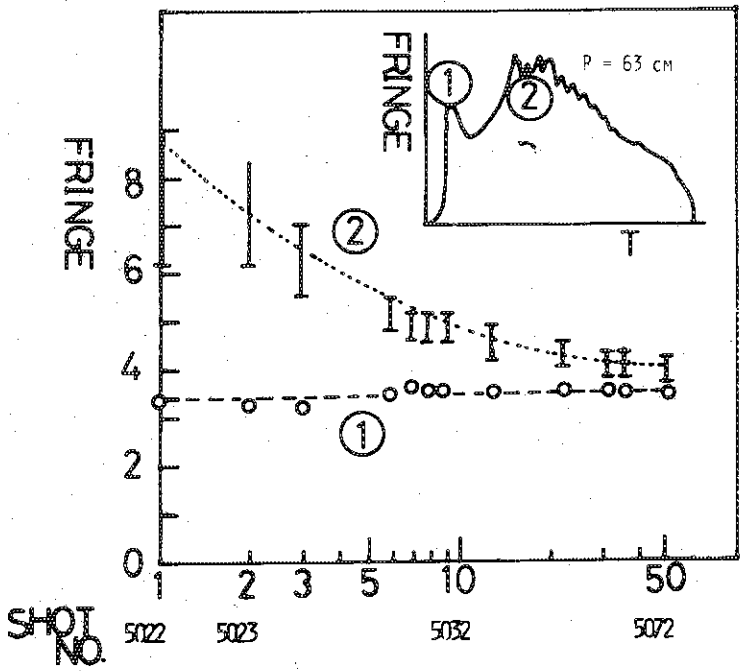

Fig. 4-2 Electron line density vs. shot-number where the discharge of No. 5022 is the first shot on a day. The operation condition is the same as in Fig. 4-1.

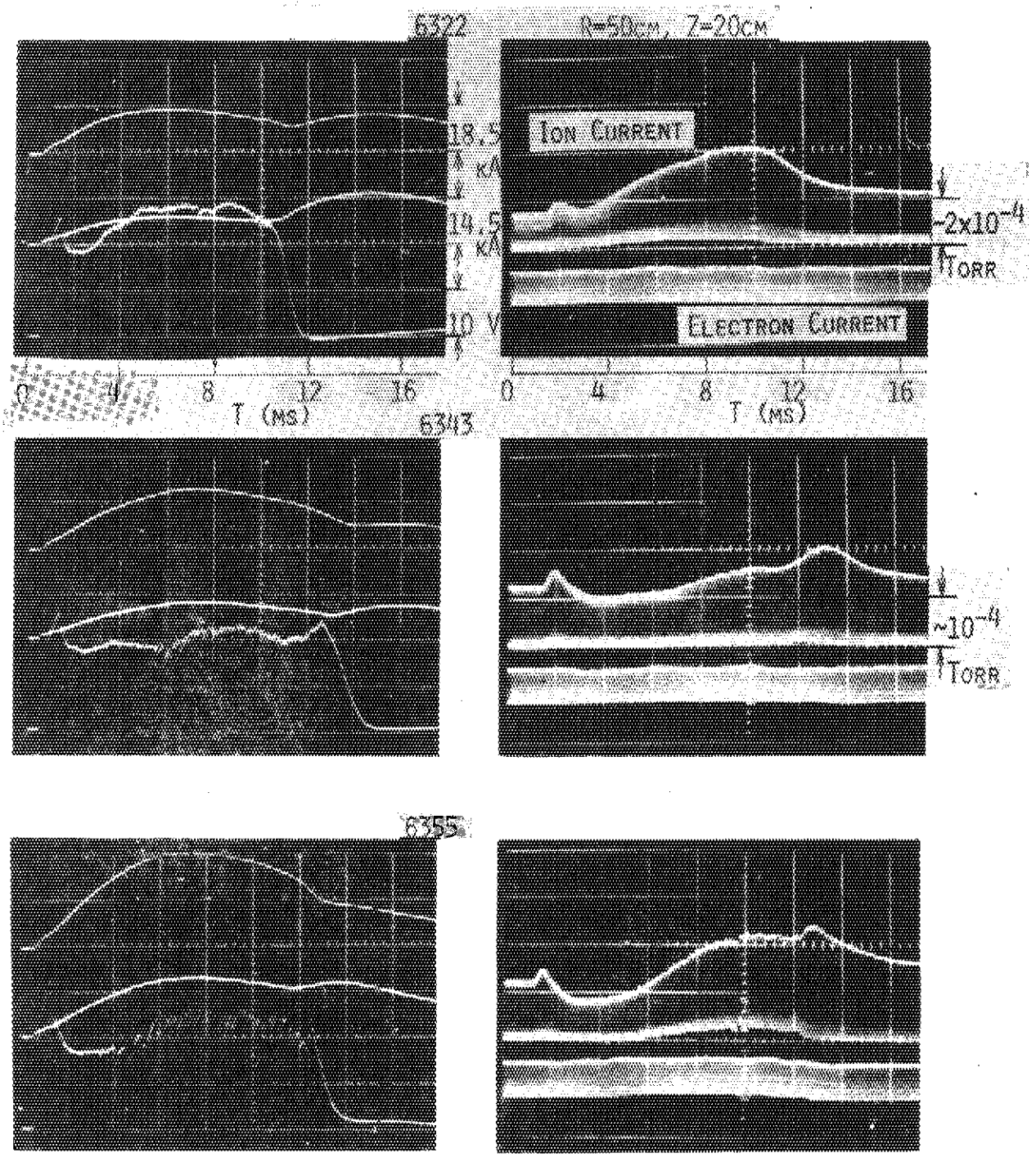

Fig. 4-3 Oscillograms of sum of plasma current I_p and divertor hoop current I_D, I_D, loop voltage V, and ion and electron currents of fast ionization gauge. The discharge of No. 6322 is the third discharge after opening the vacuum vessel to the atmosphere for about a month. The operation condiiton is the same as in Fig. 4-1.

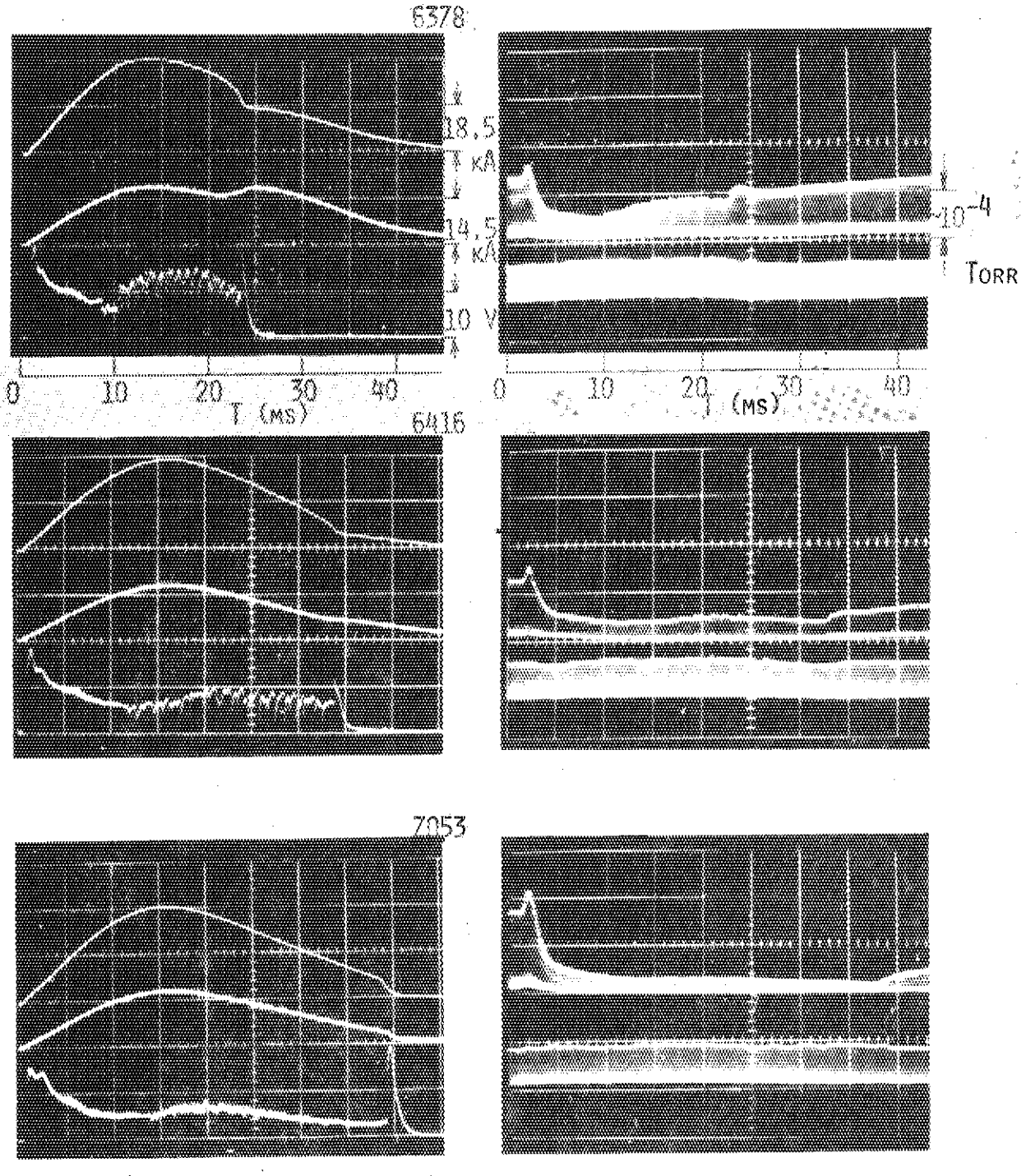

Fig. 4.3.b

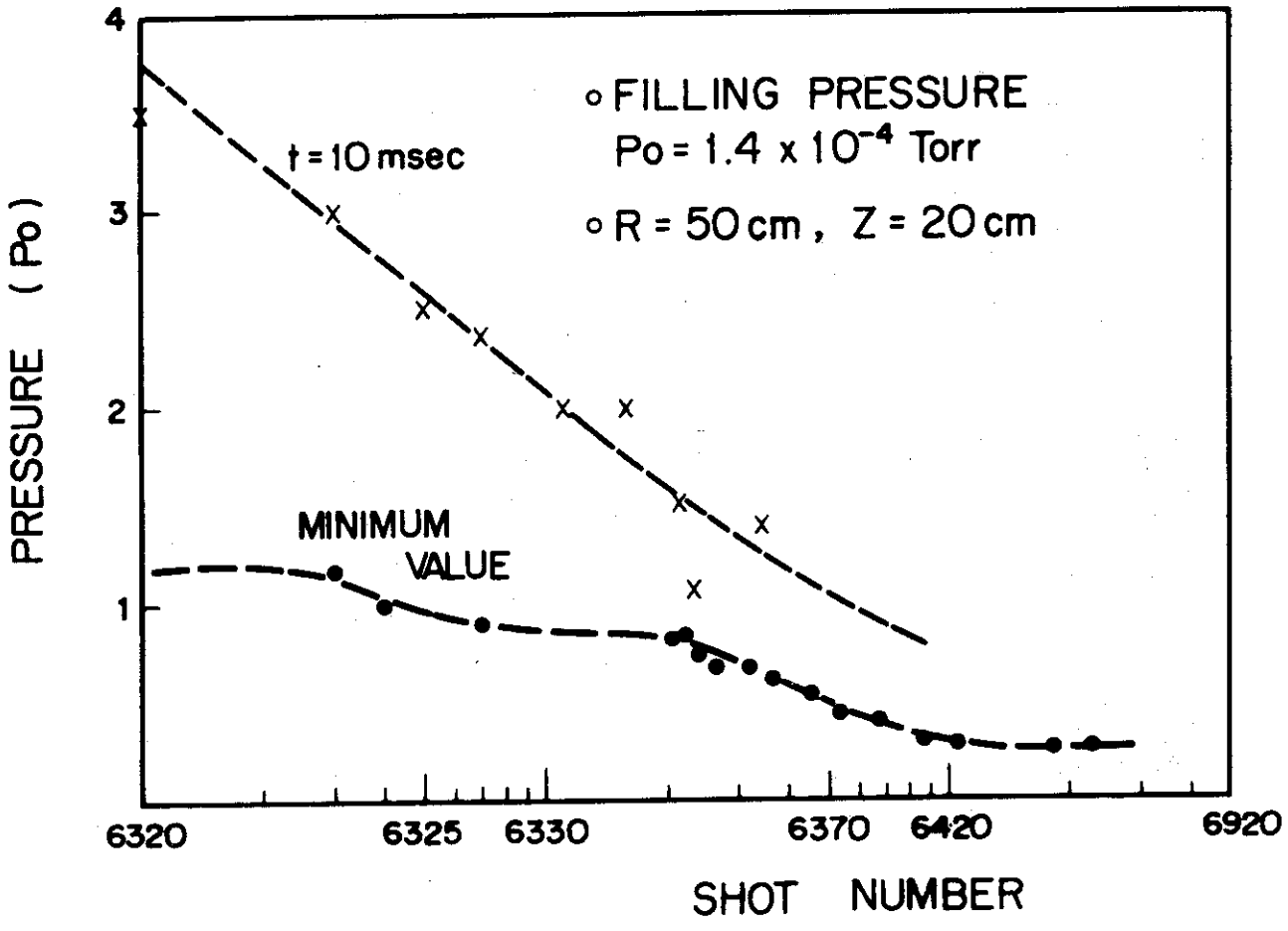

Fig. 4-4 Neutral particle pressure vs. shot-number. The discharge of No. 6320 is the first discharge after opening the vacuum vessel to the atmosphere for about a month. The operation condition is the same as in Fig. 4-1.

4.2 Characteristics of Plasmas with and without a Separatrix Magnetic Surface[1].

In this subsection, experimental results with and without exciting the divertor hoop, and some discussions concerning a separatrix magnetic surface and a magnetic limiter are presented. Discharges are obtained with the continuous gas admission.

(1) Typical Discharges at 20 kA

Figure 4-5 shows oscillograms of typical discharges at about 20 kA, which gives the q value of about 4 in a circular cross section Tokamak with a major radius of 60 cm and a minor radius of 10 cm. On the left shown are the oscillograms without a divertor hoop current (Case A) and on the right those with a divertor hoop current of 90 % of a plasma current (Case B). The gross behavior is rather similar except that the discharge lasts longer with a divertor hoop current because a plasma column shifts outward without a divertor hoop current and without a vertical field as described below. The resistivity temperature is about 70 eV at 13 ms assuming $\bar{Z} = 2$, and the average density measured by a zebra-stripe 4 mm microwave interferometer is about 1.4×10^{13} cm^{-3} at R = 63 cm. The pressure measured by a fast ionization gauge placed 10 cm from the plasma at the gap between neighboring shell sectors shows a drop from the filling pressure of 1.3×10^{-4} Torr to a plateau of 2.5×10^{-5} Torr. Negative spikes appear intermittently in the loop voltage during the discharge accompanied by a sudden increase in L_α line, C IV line (1548.2A), and density fluctuations.

The density distribution is measured by the single-channel 4 mm microwave interferometer for the main bulk of the plasma as shown in Fig. 4-6. Typical photographs of a plasma column are shown in Fig. 4-7. It is clear that a plasma of Case A shifts to outward and a plasma of Case B locates at the center of the shell except at the end of the discharge. Except the positions of plasmas, the characteristics of density distribution and time variations of Case A and Case B are similar for the initial 15 ms. Figure 4-8 shows the magnetic field distribution measured by magnetic probes placed on the inner surface of the shell. For comparison, also shown in the figure are the calculated poloidal field distributions for a uniform current distribution of two values of β_p. It is shown that the measured magnetic field distribution agrees with the case of $\beta_p = 0.1$ whose equilibrium configuration is shown in Fig. 4-9. However, the

agreement does not necessarily exclude other current distributions and other values of β_p.

The density distribution of the outskirt of the plasma is measured with double probles. Figure 4-10 shows the typical waveforms of ion saturation currents near the divertor hoop (R = 40 cm and Z = -3.75 cm) and near the inner surface of the shell (R = 68 cm and Z = -6.2 cm). It is shown that the ion saturation current of Case B near the divertor hoop is about 10^3 times larger than that of Case A except at the beginning of the discharges. The density profile near the divertor hoop measured by scanning a double probe (Fig. 4-11) shows a peak at Z = -3 cm, suggesting the presence of the plasma extending towards the divertor near the separatrix magnetic surface. The electron temperature is about 10 eV and the maximum plasma density is about 1×10^{12} cm^{-3} at 13 ms. The density profile near the inner surface of the shell by scanning a double probe (Fig. 4-12) shows that the ion saturation current with a separatrix magnetic surface is less than that without a separatrix magnetic surface only at the beginning of a discharge.

The full profile of the ion saturation current near the divertor hoop is shown in Fig. 4-13 for Case B. It is clear that the profile has asymmetry as to the median plane. The larger peak always locates at 3 cm from the median plane to the direction of electron drift even when the direction of toroidal field and/or plasma current are varied. It is considered that radial and/or toroidal electric field and toroidal magnetic field cause this asymmetry[11].

Figure 4-14 shows oscillograms of typical discharges with a divertor hoop current of 45 % of a plasma current (Case C). In this case, the gross behavior of a main plasma is similar to that of Case B but the ion saturation current near the divertor hoop is about 10^{-2} times less than that of Case B except at the beginning of a discharge. In Fig. 4-14, the ion saturation current only at R = 40 cm and Z = -2 cm is shown and is similar to those at other positions (R=40 cm and Z=-3~+3 cm).

(2) Typical Discharges at Higher and Lower Currents

Figure 4-15 shows oscillograms of discharges of 20 kA, 25 kA and 30 kA with a divertor hoop current of 90 % of a plasma current. It is indicated that the plasma is unstable with a plasma current more than 20 kA and the current does not increase any more than 30 kA. Figure 4-15, shows negative spikes occurring in the discharge of 25 kA together with the

corresponding fluctuations of poloidal magnetic field. It is observed that fluctuations of poloidal field at frequency of about 20 kHz are excited[12], the amplitude of the fluctuations increase until a negative spike apears as shown in Fig. 4-16. In the discharge at a current lower than about 15 kA, distruptive fluctuations in the one turn voltage, electron density and line radiation are greatly reduced.

(3) Discussions

It is interesting to know whether a plasma enclosed in a separatrix magnetic surface is produced or not in this device. In the case of $I_D/I_p = 0.9$ (case B), a plasma of the density of 1×10^{12} cm^{-3} is observed and, in the case of I_D/I_p (Case C), very little plasma is observed except at the beginning of a discharge. These experimental results are consistent with calculated results. In the Case B, it is clear that a plasma enclosed in a separatrix magnetic field is produced and the plasma extends to the divertor region approximately along the magnetic surfaces. At the beginning of a discharge in all cases, plasma may be produced near the divertor hoop because of high pressure, large one turn voltage and small rotational transform, and rather large ion saturation current are observed near the divertor hoop as shown in Figs. 4-10, 4-11 and 4-14.

The experimental results described above indicate that, in the gross behavior of the plasma, there are no significant differences whether or not the plasma is enclosed in a separatrix magnetic surface. It is also indicated that the MHD behavior of a plasma with a teardrop-like cross section with a separatrix magnetic surface is similar to that of a conventional Tokamak. Numerical calculation about localized mode also shows that the current density limit of this device with large aspect ratio is not largely different from that of a conventional Tokamak. Further detailed investigation is needed concerning this behavior, but it can be said that no adverse effects of the separatrix magnetic surface on the plasma confinement are obserbed. This result encourages the attempt to reduce impurity content in a confined plasma by an axisymmetric divertor.

Preliminary results suggest that the plasma flow to the divertor region is not dominant in these discharges because there are no significant differences whether or not the plasma is enclosed in a separatrix magnetic surface. In ref. (2), the particle flux to the divertor was estimated assuming a mirror loss in which the particle flux is determined by the collisional frequency and not by the flow velocity of each particle.

In the discharges described above, the collisional time is less than 10 μs assuming ion temperature less than electron temperature and flow time of the plasma along the magnetic field from the confinement region to the divertor region is 50 μs or more assuming the flow velocity is 0.5 × (sound velocity). Therefore, the estimation shown in ref. (2) is not reasonable in these discharge. Another estimate applicable in cases where the flow velocity along magnetic field lines and particle diffusion across magnetic field lines are described bellow. If the following equation is satisfied, most of particles lost from the confinement region reaches the divertor region.

$$x_b >> \sqrt{\tau_f D} \equiv x_D,$$

where x_b is the distance between the confined plasma and the wall, D is a particle diffusion coefficient and τ_f is expressed by the following equation.

$$\tau_f \simeq \pi R\bar{q}/V_f,$$

where V_f is the flow velocity along the magnetic field lines. Assuming V_f = 0.5 × (sound velocity) and D = (anomally factor) × (neoclassical diffusion coefficient), x_D is expressed by the following equation for a hydrogen plasma with $\bar{q} \simeq 2$ and R = 60 cm.

$$x_D \simeq 4 \times 10^{-8}\sqrt{\gamma \bar{q}^3[n(cm^{-3})][T_e(eV)]^{-1}}/B_T(T)\,cm$$

For the Case B at 13 ms, $x_D \simeq 0.2\sqrt{\gamma}$ cm and x_b < 1 cm. Assuming $\gamma \gtrsim 100$, larger part of particles lost from the confinement reaches not to the divertor region but to the wall. Assuming the flow velocity, the experimental particle flow to the divertor region is about 3.5×10^{16} (particles/ms) at 13 ms in Case B and the particle loss flux from the confinement is $1.5 \times 10^{18}/\tau_n$ at the same time where τ_n is particle confinement time. τ_n has not been measured but must be smaller than 10 ms. From these estimations, it can be said that most of the particles lost from the confinement reaches not to the divertor region but to the wall in these discharge.

In order to realize an effective magnetic limiter and/or divertor, it is necessary to increase the particle flow F_D to the divertor and to decrease the particle flow F_W to the wall. It is considered to be resonable that F_D/F_W is small in JFT-2a with the small dimensions and a weak toroidal field. F_D/F_W may be increased effectively by increasing the intensity of

the toroidal field but the maximum intensity of the toroidal field is 1 T in JFT-2a. Other possibilities of increasing F_D/F_W are discussed below.

F_D/F_W increases as increasing rotational transform or plasma current following the estimation described above. Experimental results show that the plasma is unstable with a plasma current more than 20 kA and it can be said that it is impossible to increase largely F_D/F_W by large increasing rotational transform in a stable discharge.

The flow velocity to the divertor region and particle confinement time may be increase as increasing plasma temperature and as decreasing plasma density. It is under preparation to investigate these possibilities by reducing a greater part of neutral particles around a plasma by using fast acting valves and flushing titanium.

It is prepared to increase the distance from confined plasma to the wall by increasing a divertor hoop current.

It is also shown that electric field rules the plasma behavior near the separatrix magnetic surface.

Further detailed investigation is needed concerning the particle and heat flux to the divertor region, particle and energy confinement time, electron and ion temperature and impurity contents.

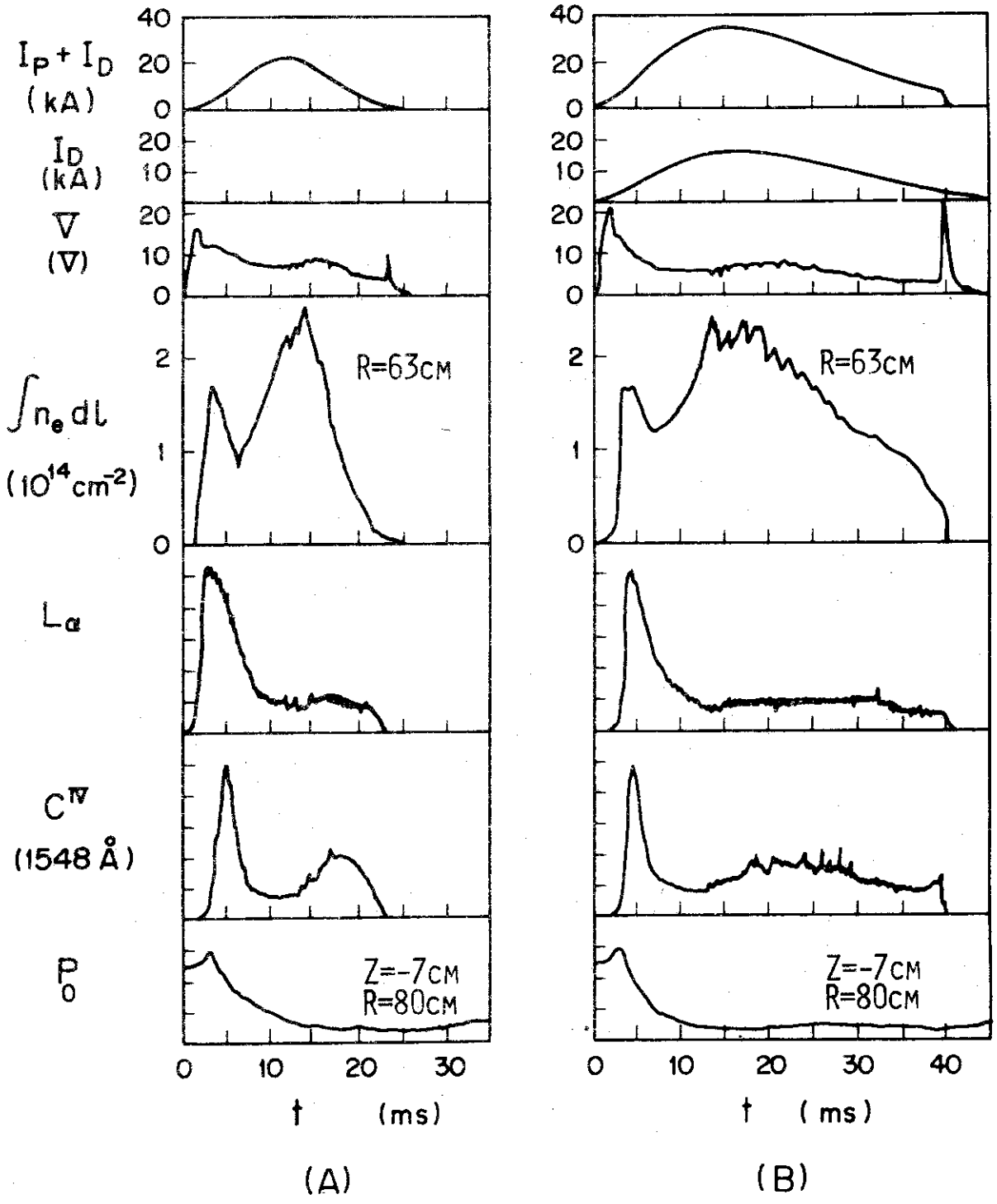

Fig. 4-5 Oscillograms of sum of plasma current I_p and divertor hoop current I_D, I_D, electron line density, light intensities of L_α and CIV lines, and neutral particle pressure P_o at the gap of neighboring shell sections. Case A is for I_D/I_p=0 and Case B for I_D/I_p=0.9. The operation condition is B_v=0 and the continuous filling pressure 1.3×10^{-4} Torr.

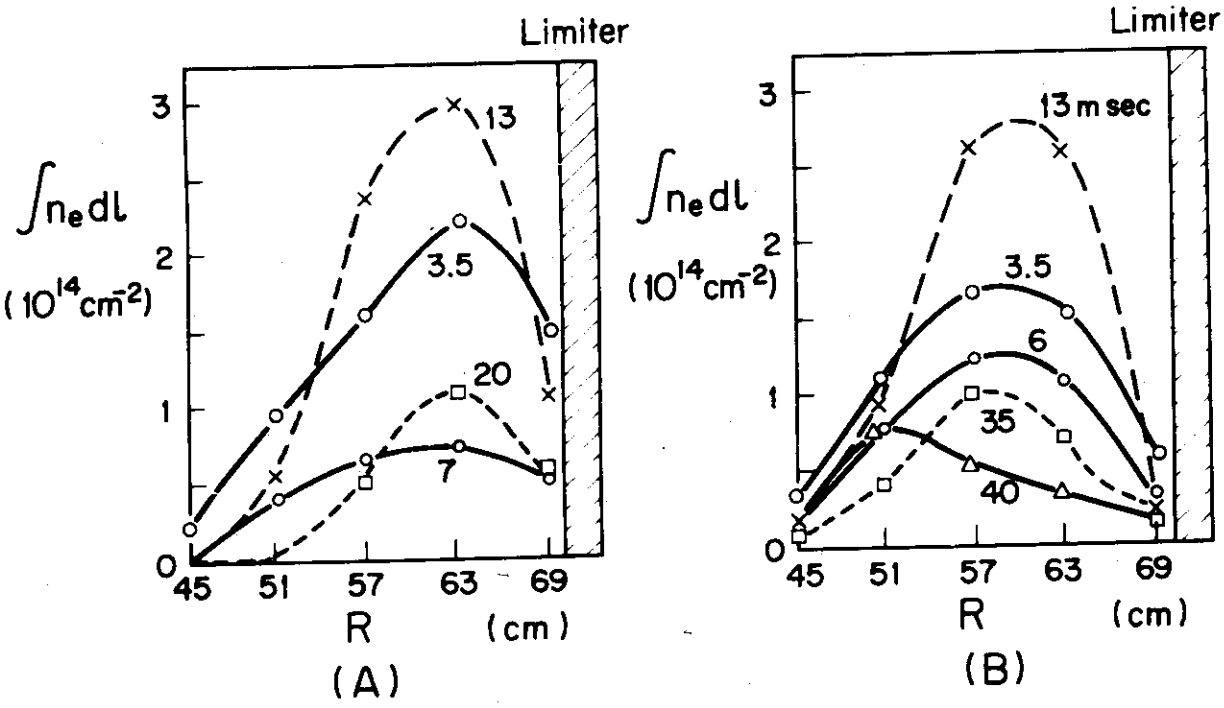

Fig. 4-6 Time variation of electron line density distribution. The operation condition is the same as in Fig. 4-5.

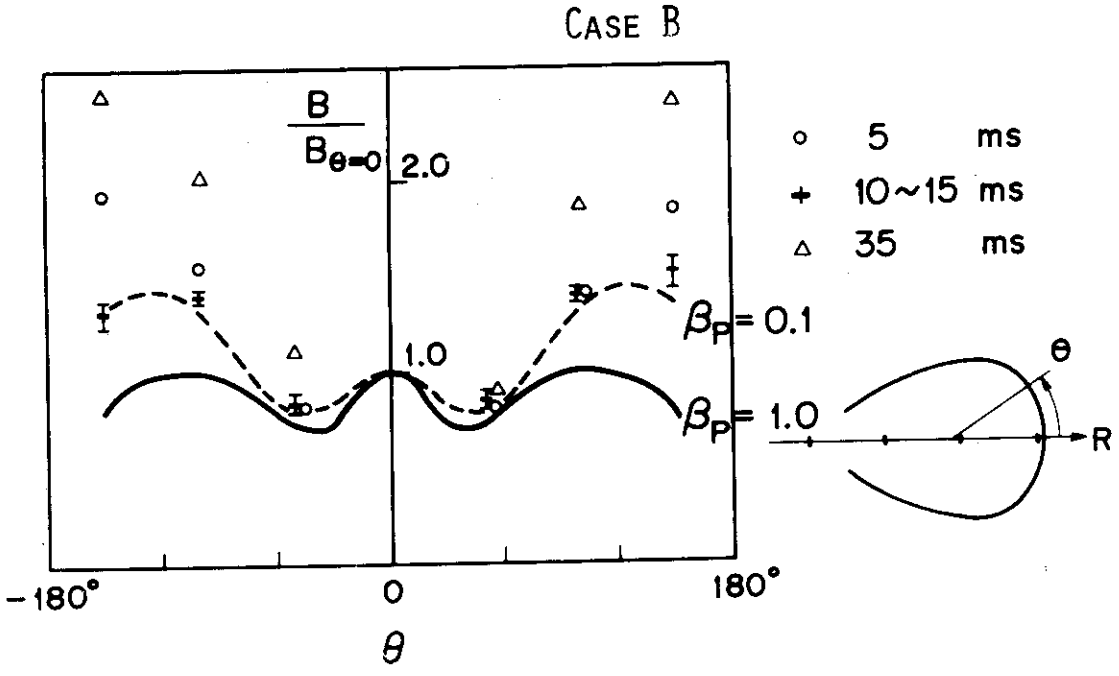

Fig. 4-8 Poloidal magnetic field distribution on the inner surface of the shell measured by magnetic probes for Case B. Curves show calculated results for a uniform current distrubition with β_p=1 and 0.1. The operation condition is the same as in Fig. 4-5.

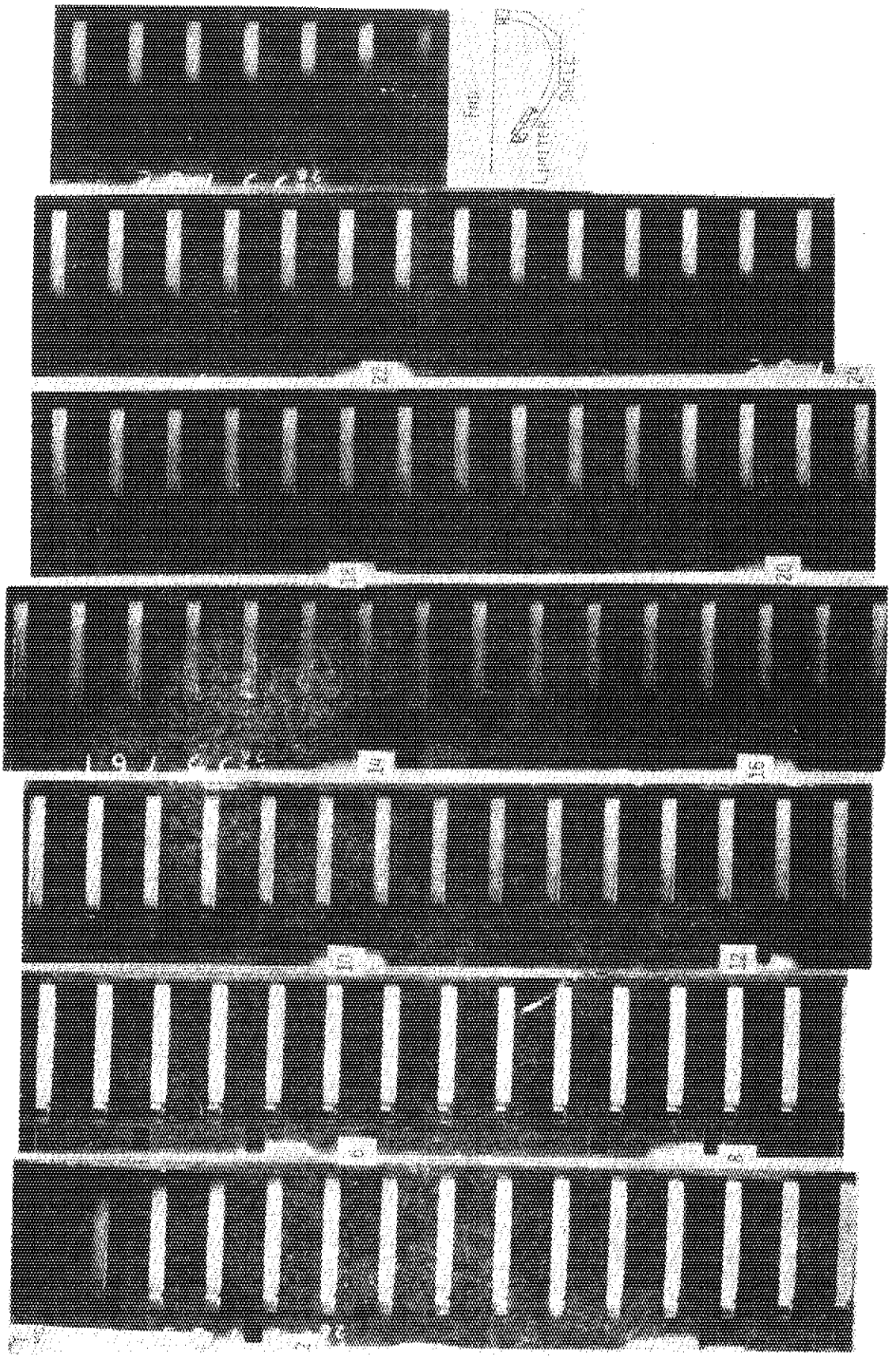

Fig. 4-7 Photographs of plasma column. The operation condition is the same as in Fig. 4-5.

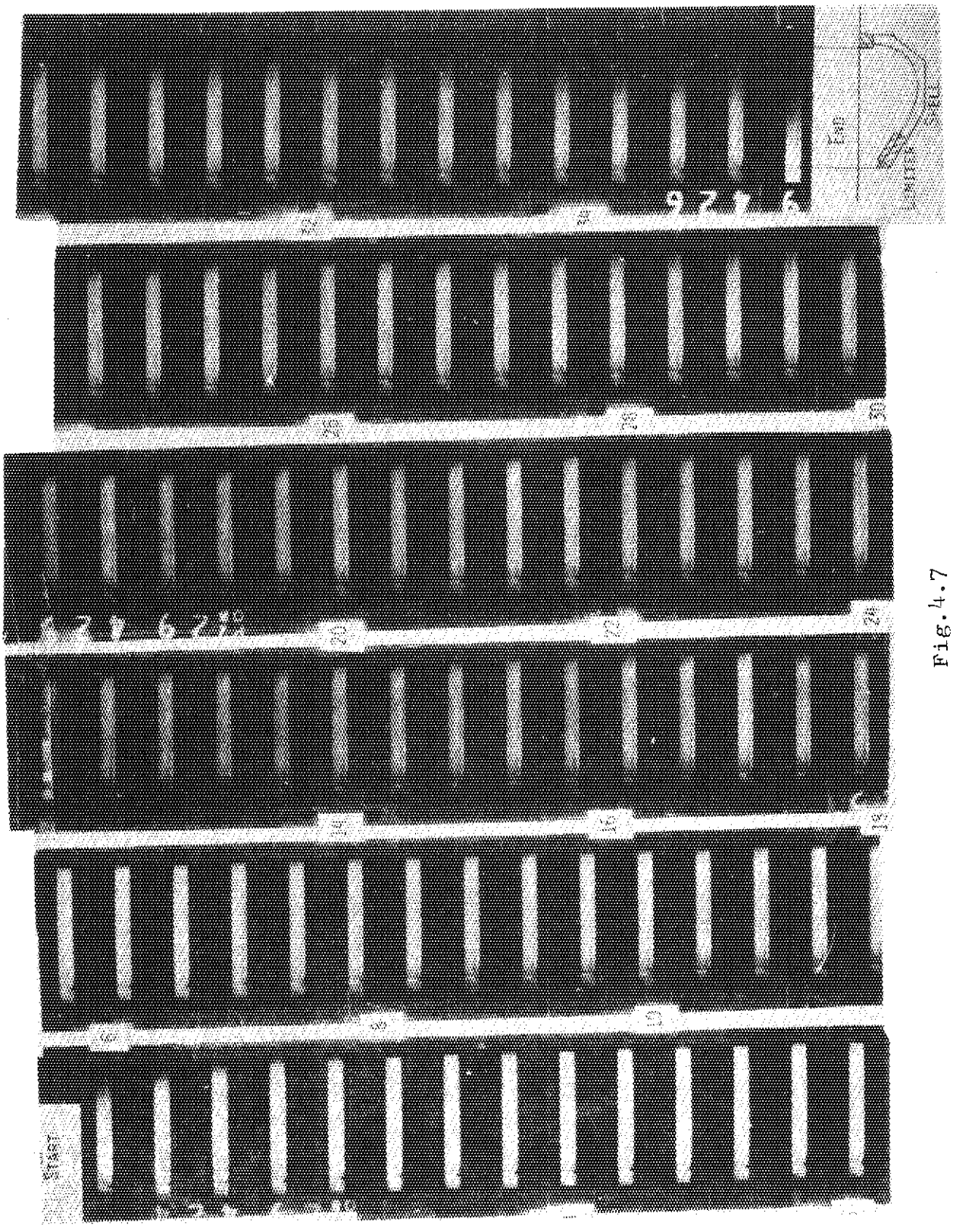

Fig.4.7

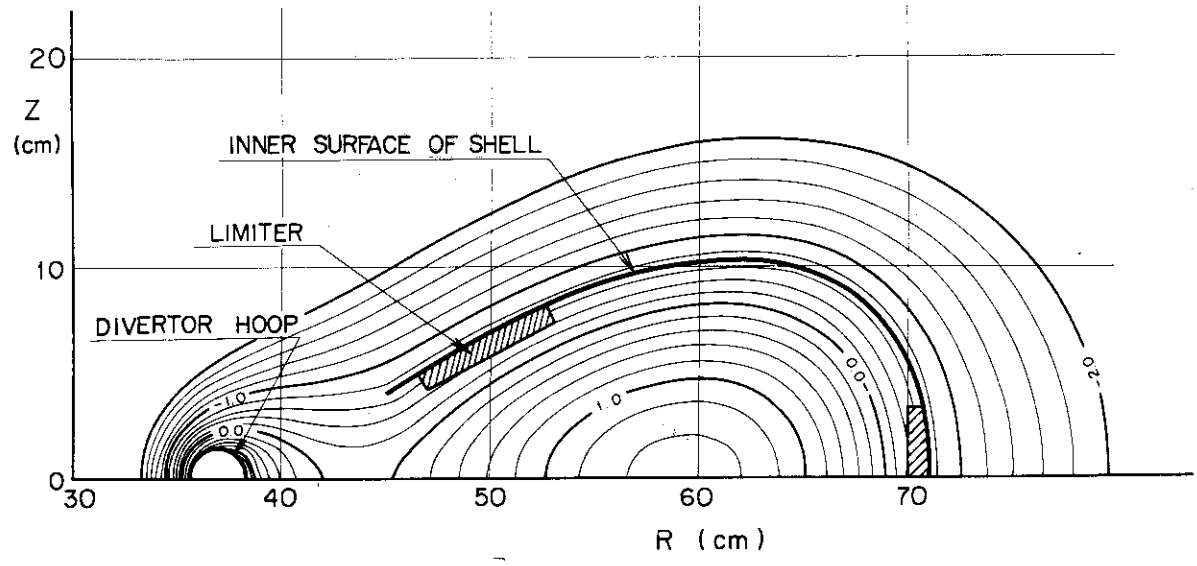

Fig. 4-9 An example for an equilibrium configuration of univorm current distribution, β_p=0.1 and I_D/I_p=0.9, obtained by numerical calculation.

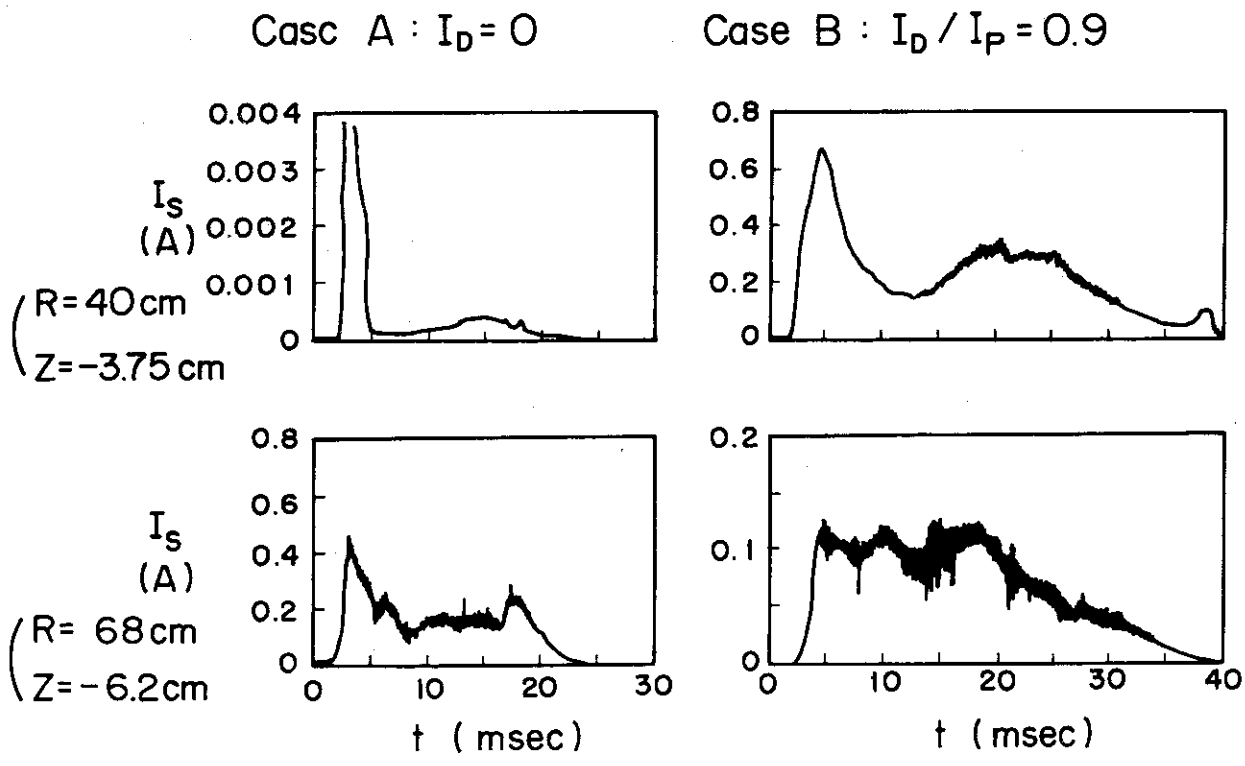

Fig. 4-10 Oscillograms of double probe current near the divertor hoop (R=40cm, Z=-3.75cm) and near the inner surface of the shell (R=68cm, Z=-6.2cm). The operation condition is the same as in Fig. 4-5.

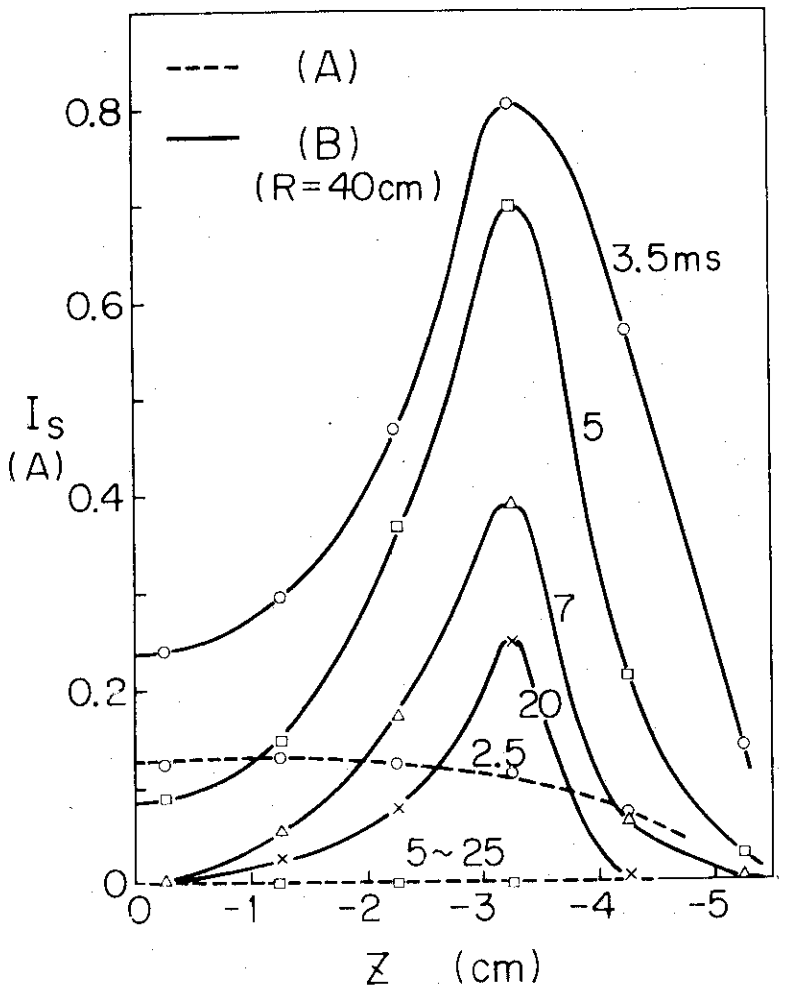

Fig. 4-11 Double probe current near the divertor hoop vs. vertical distance from the median plane. Direction of electron drift is antiparallel to Z axis. The operation condition is the same as in Fig. 4-5.

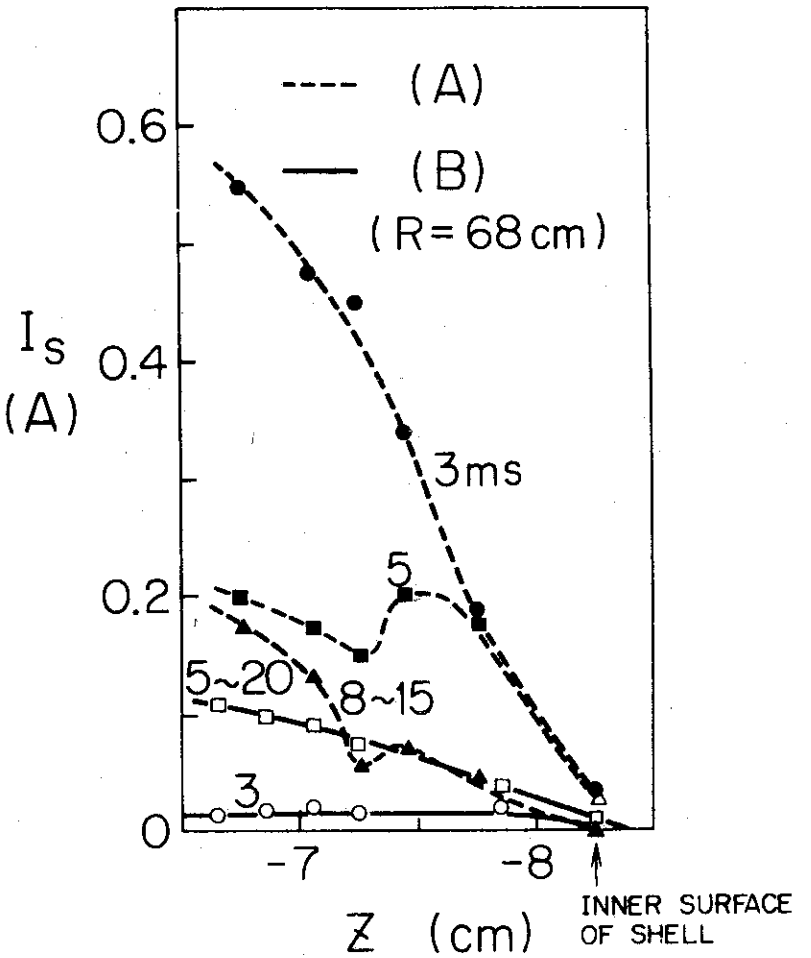

Fig. 4-12 Double probe current near the inner surface of the shell vs. vertical distance from median plane. Direction of electron drift is antiparallel to Z axis. The operation condition is the same as in Fig. 4-5.

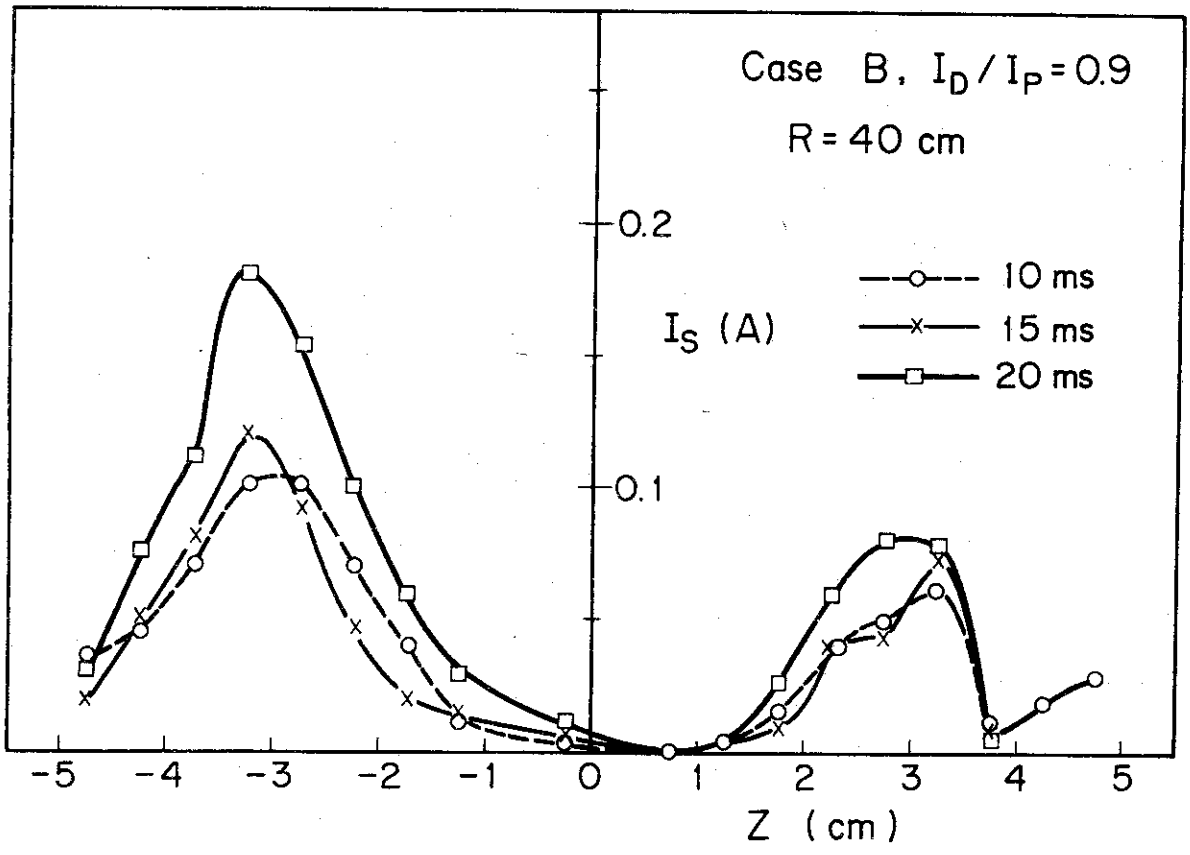

Fig. 4-13 Double probe current near the divertor hoop vs. vertical distance from the median plane. Direction of electron drift is antiparallel to Z axis. The operation condition is similar to that shown in Fig. 4-5.

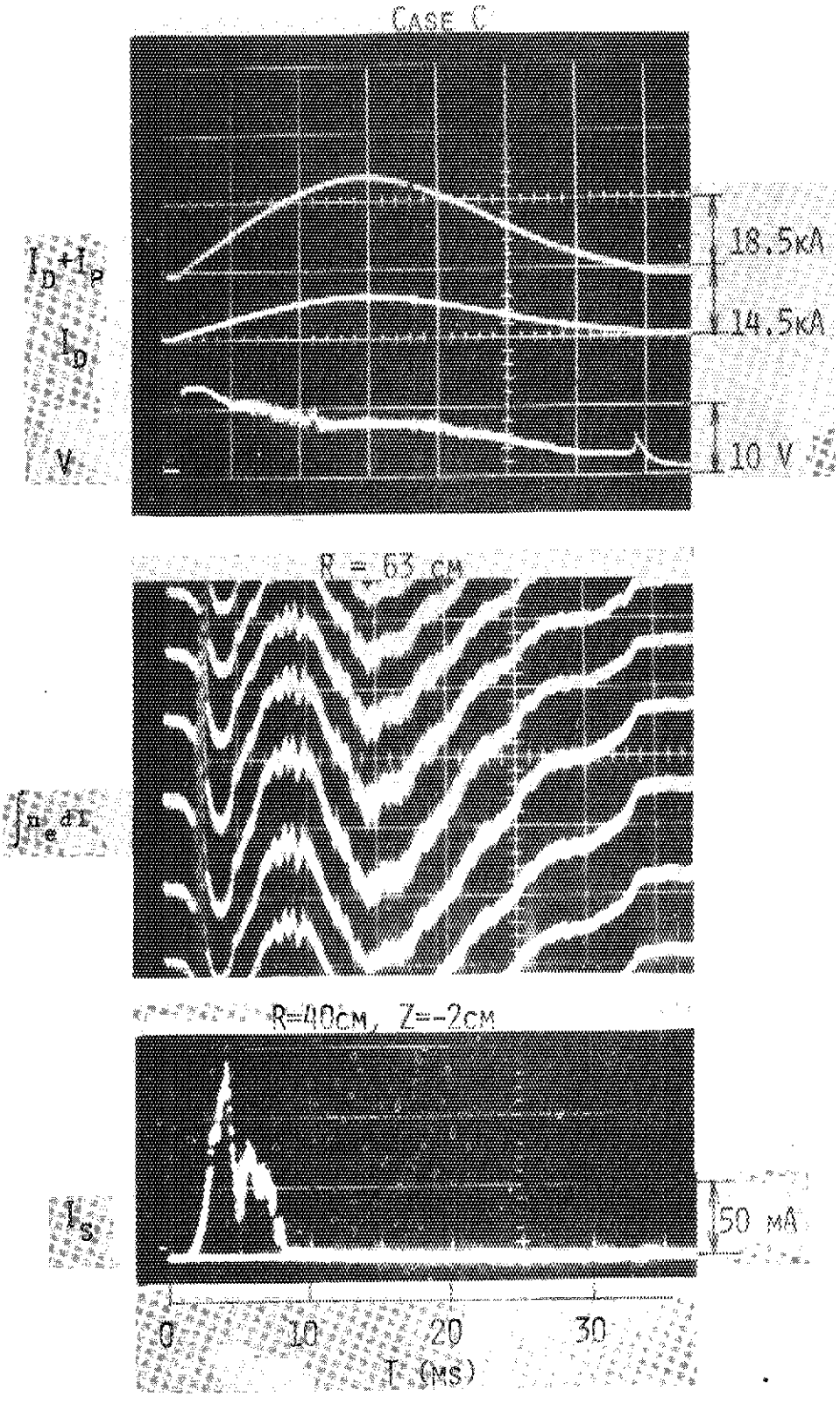

Fig. 4-14 Oscillograms of sum of plasma current I_p and divertor hoop current I_D, I_D, loop voltage V, electron line density, and double probe current near the divertor hoop. The operation condition is I_D/I_p=0.45, B_V=0 and the continuous filling pressure = 1.3×10^{-4} Torr.

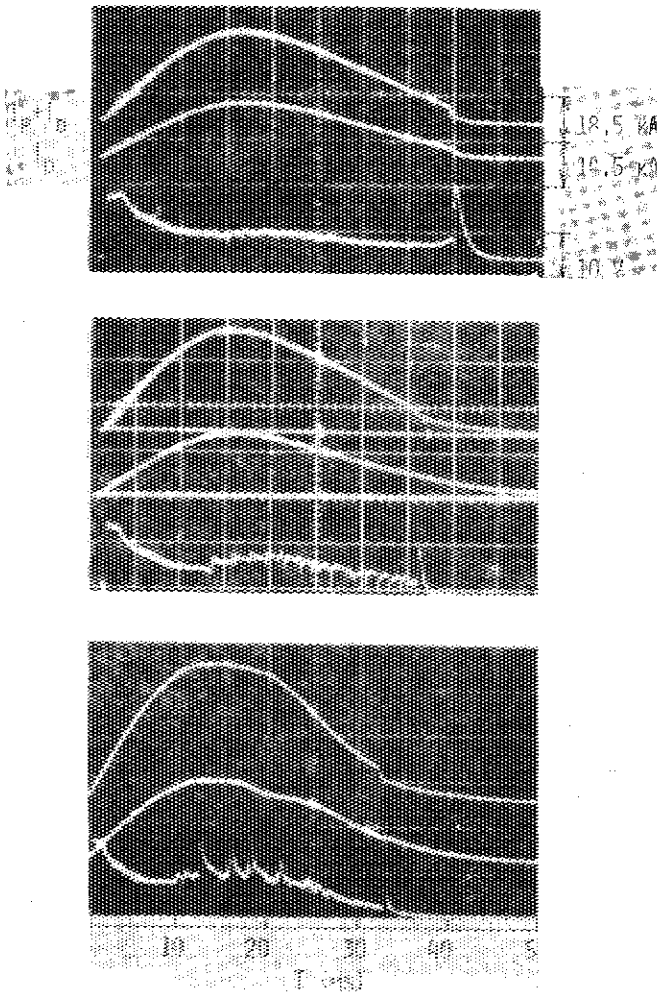

Fig. 4-15 Oscillograms of sum of plasma current I_p and divertor hoop current I_D, and loop voltage V. The operation condition is I_D/I_p=0.9, B_V=0 and continuous filling pressure = 1.3×10^{-4} Torr.

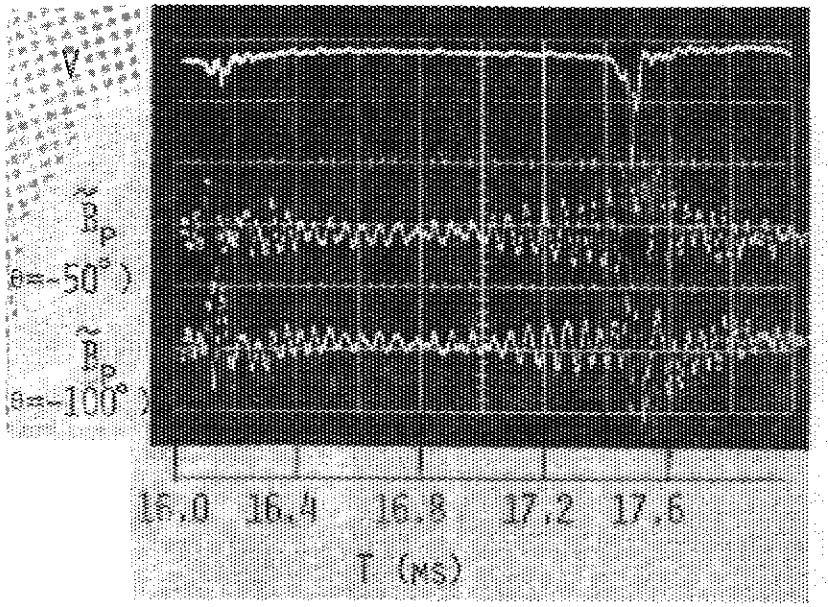

Fig. 4-16 Oscillograms of fluctuations of loop voltage V and poloidal filed $\tilde{B}_p$. The operation condition is similar to that shown in Fig. 4-5 and the maximum plasma current is about 25 kA.

4.3 Plasma Density and Neutral Particle Density

To start discharges as soon as possible after admitting hydrogen gas by four fast acting gas valves of variojs plenum pressure, large one turn voltage in the early phase of discharges is obtained by using two condenser banks. These two condenser banks are discharged one after the other as described in 2.5 and supply a large one turn voltage of about 100 V in the early phase of a discharge and sustain a plasma current at a constant value for several milliseconds. Four fast acting gas valves are sxisymmetrically located as shown in Fig. 2-3 and supply hydrogen gas directly into the shell. In this subsection, discharge characteristics concerning plasma and neutral particle density under various discharge conditions are described.

(1) Experimental Data[13)]

Figure 4-17 shows oscillograms of typical discharges using two condenser banks. The discharge starts at 0.8 ms after driving four fast acting valves, a plasma current reaches the maximum value at 1.2 ms after starting the discharge, and the one turn voltage and the plasma current are sustained at the constant value for 7 ms. The resistivity temperature is about 100 eV for this period assuming $\bar{Z} = 2$ and uniform distribution. Plasma density reaches the first peak value at about 1.5 ms. In Fig. 4-17, neutral particle density outside of the shell (R=50cm and Z=20cm) is also shown. The discharge starts at the time when the pressure at R = 50 cm and Z = 20 cm reaches one third of the mean filling pressure in the vacuum chamber. Neutral particle density at this position reduces during the discharge and reaches the value less than one tenth of the mean filling pressure at the end of the discharge.

The time variation of the electron line density distribution and total electron number is shown in Fig. 4-18 with various discharge conditions, using fast acting gas valve and $I_D/I_p = 0.9$ (Case (FB)), using continuous leak valve and $I_D/I_p = 0.9$ (Case (CB)), using fast acting gas valves and $I_D = 0.0$ (Case (FA)). It can be seen that there are no significant differences among those cases shown in Fig. 4-18 except the position of the density peak shifts outward in Case (FA) without exciting the divertor hoop as described in 4.2. In all of those cases, the density distribution becomes sharp, then negative spikes appears and the plasma column spreads. In the cases with $I_D/I_p = 0.9$, the total number of electrons at the first density peak is equal to the total number of atoms

admitted in the shell. The value of the first density peak is constant even if a plasma current varies from 12 kA to 27 kA.

In Fig. 4-19, the time variation of the total number of electrons and neutral particles are shown. The total number of neutral atoms is calculated from the pressure at R = 50 cm and Z = 20 cm assuming that the density of neutral particles is uniform outside of the shell. It is shown that the sum of atoms and electrons is reduced after 10 ms and is only one twenty-fifth the number of the atoms admitted. The total number of atoms in the vacuum chamber increases in the time constant of several seconds after discharge.

Figure 4-20 shows the relation between the line electron density at the first peak and filling pressure and it is shown that a plasma with various density can be obtained.

(2) Discussion

By using fast acting gas valves and applying large one turn voltage, most of the particle admitted are ionized and trapped at about 2.3 ms after driving the fast acting gas valves and the number of the remaining neutral particles outside of the shell is about one sixth of that of admitted gas at the same time if we assume that the neutral particle density is uniform outside of the shell. The total number of electrons at the first density peak is equal to the total number of atoms admitted in the shell but the total number of electrons at the second peak varies with discharge conditions in which the filling pressure is remained constant value as shown in 4.1. It may be noted here that the interactions between the walls and a plasma plays a dominant role in the later part of discharge.

Not only the total number of neutral particles but also the sum of that and electrons is reduced after 10 ms and it is clear that the atoms admitted in the vacuum chamber are absorbed to the wall during the discharge. These absorbed particles are released long after the discharge and desorbing time constant is several seconds. It has not been investigated which surface plays important role in this phenomenon.

It is interesting that the total number of electrons is roughly constant for several milliseconds but it is not clear what kind of particle recycling processes plays important role. Particle influx from outside of the shell is estimated to be less than 3×10^{16} (particles/ms) at 10 msec assuming that hydrogen molecules spread into the shell with

thermal velocity of 300 °K. Particle flux due to the thermal desorption is estimated to be less than 10^{15}(particles/ms) at the same time from Fig. 4-19. Sum of these flux is much less than the total particle loss flux of plasma which is 1.5×10^{17} (particles/ms) even if we assume that particle confinement time is 10 ms. By this reason it is reasonable to consider that other recycling process is important in this device.

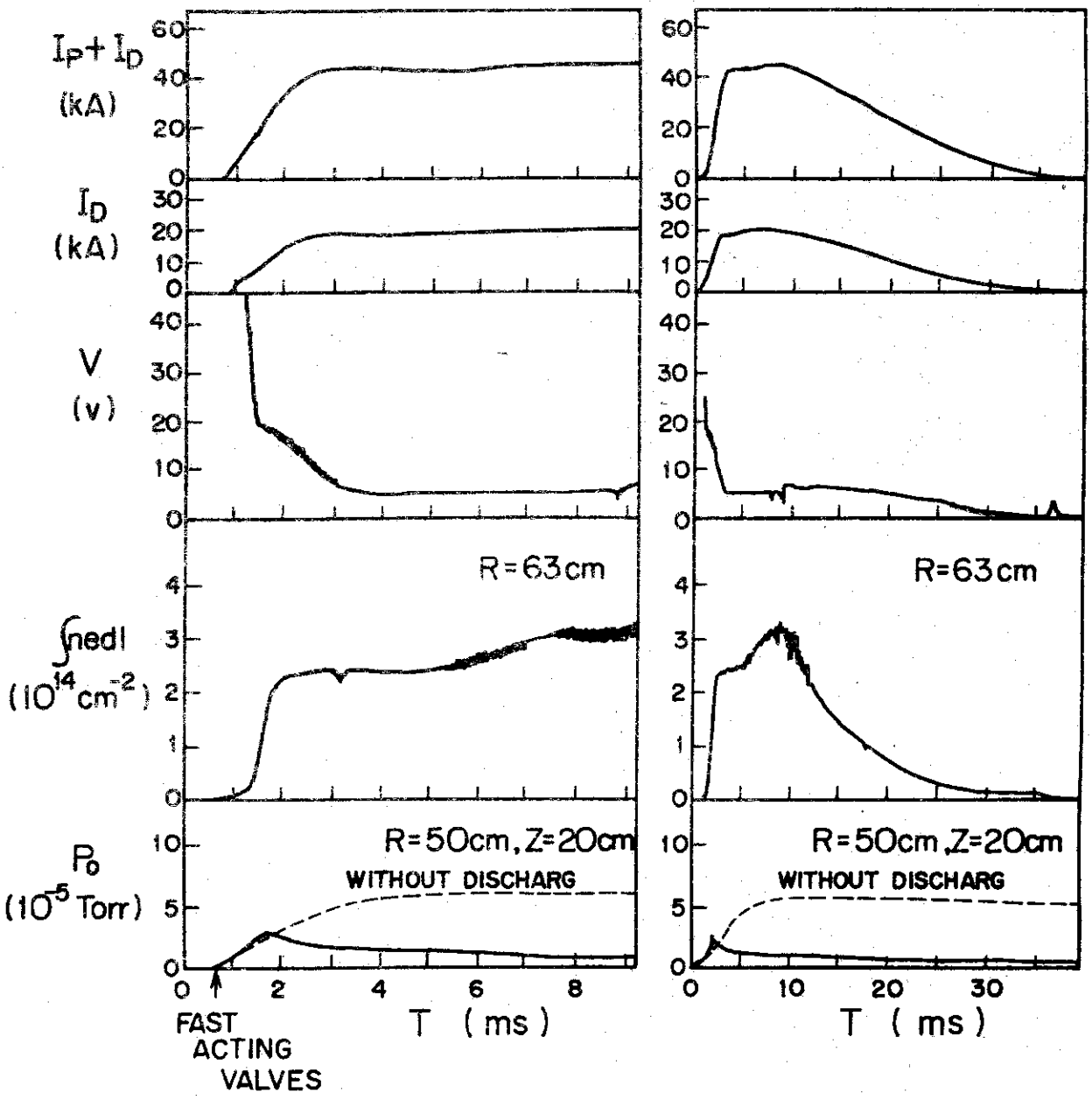

Fig. 4-17 Oscillograms of sum of plasma current I_p and divertor hoop current I_D, I_D, loop voltage V, electron line density, and neutral particle pressure P_o. The operation condition is $I_D/I_p=0.9$, $B_v=0$ and the working gas admitted by four fast acting gas valves.

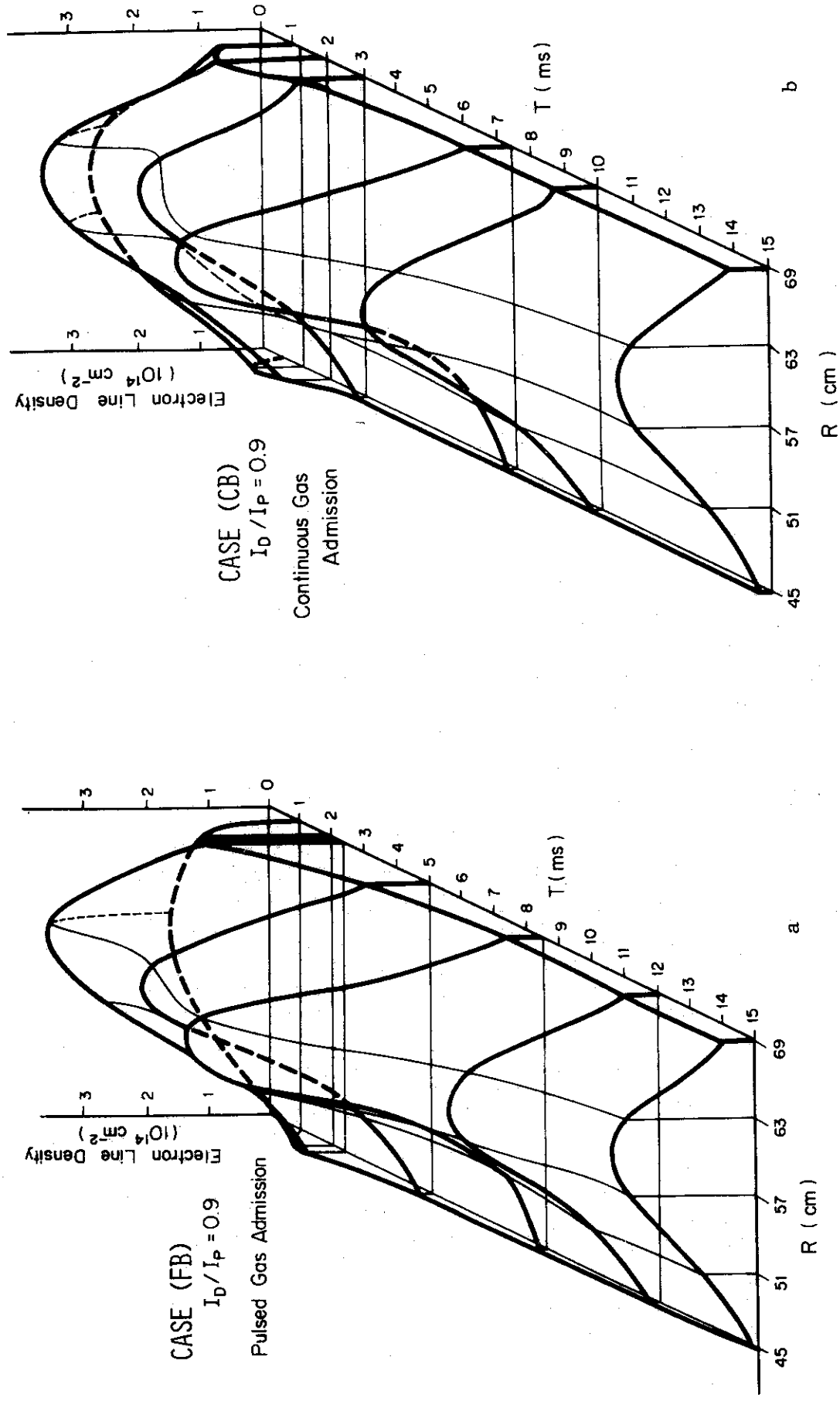

Fig. 4-18 Electron line density distribution and total number of electrons. The maximum plasma current is about 20 kA.

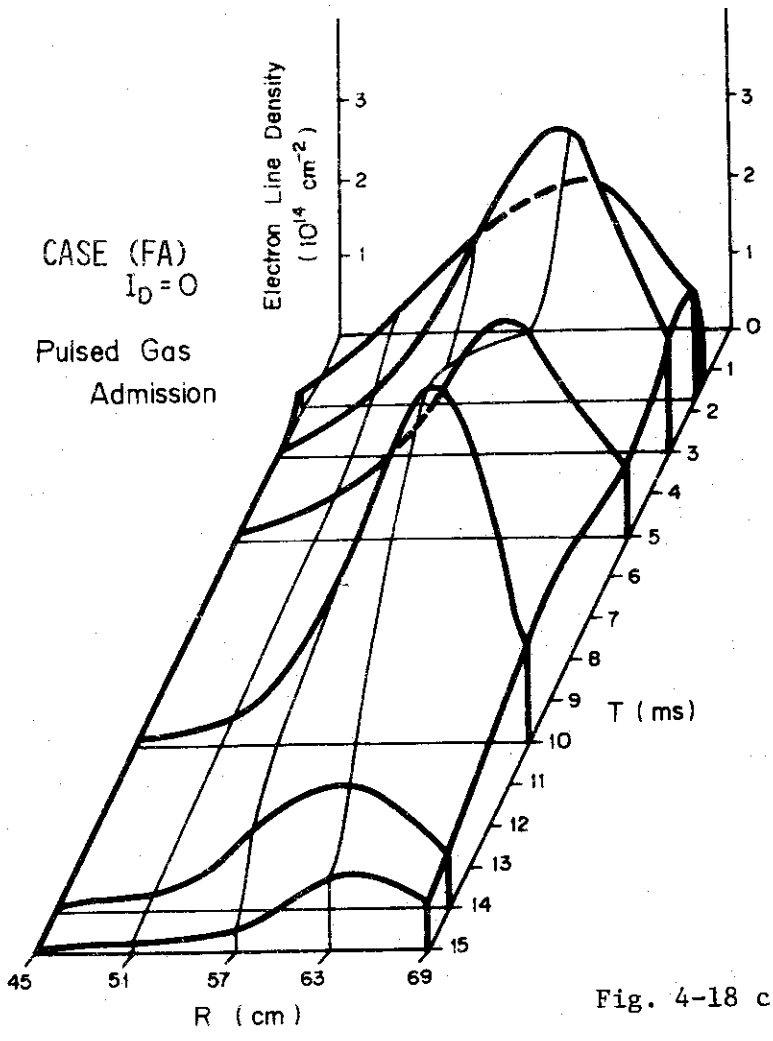

Fig. 4-18 c

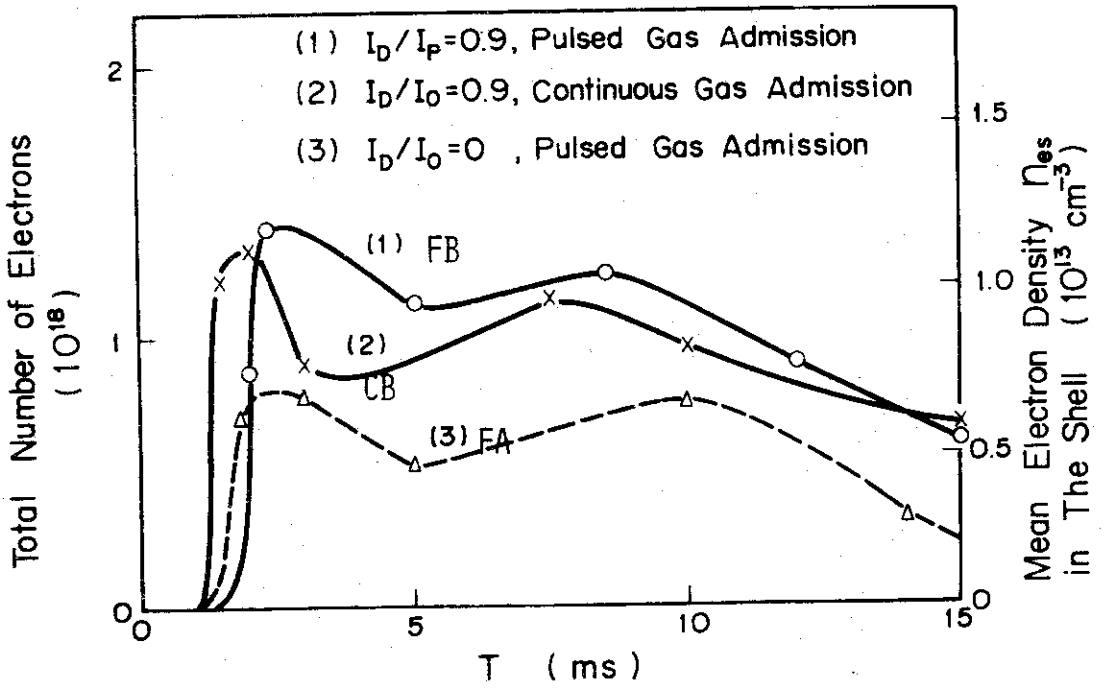

Fig. 4-18 d

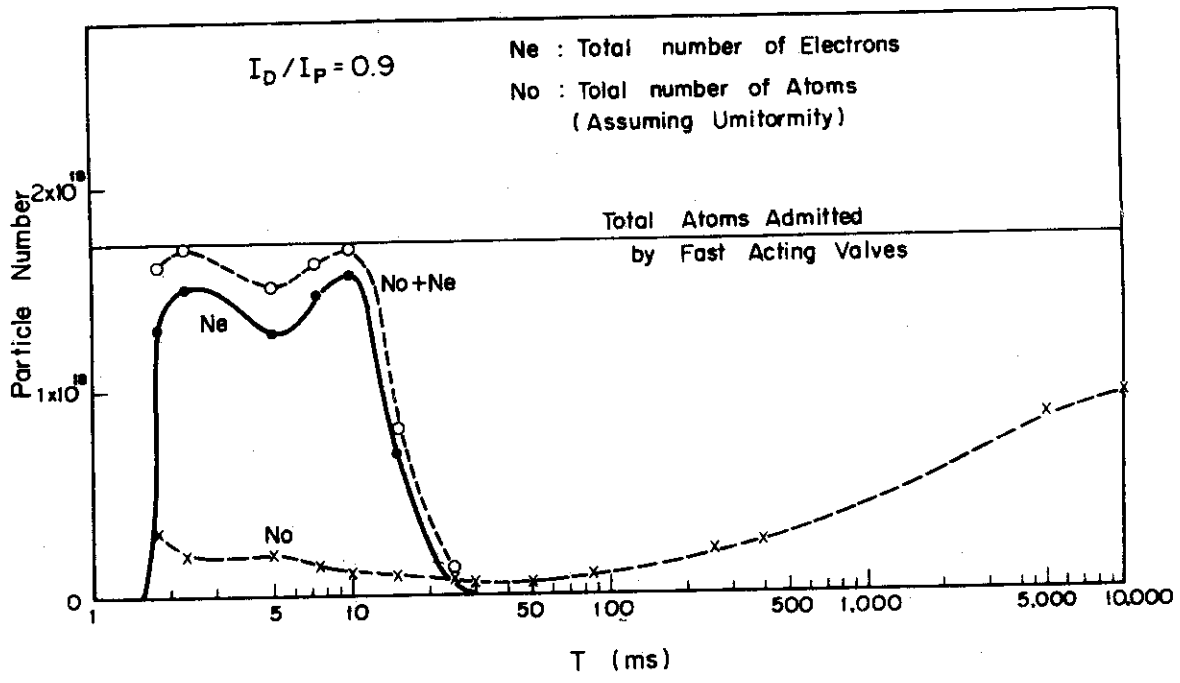

Fig. 4-19 Total number of electrons and neutral particles. The discharge condition is the same as in Fig. 4-17.

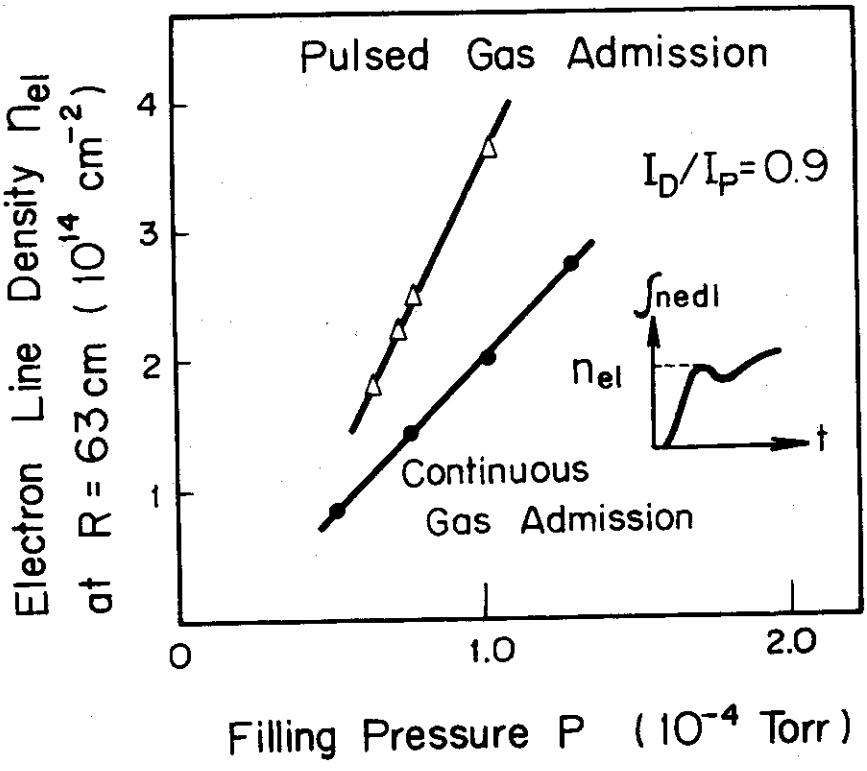

Fig. 4-20 Electron line density vs. filling pressure. The maximum plasma current is about 20 kA and the operation condition is I_D/I_p=0.9 and B_v=0.

5. Summary

JFT-2a (DIVA) with a teardrop-like cross-section capable of operating an axisymmetric magnetic limiter and/or divertor was constructed and the device was put into operation in September 1974.

Preliminary measurements indicate that a plasma enclosed in a separatrix magnetic surface is obtained and no adverse effects of the separatrix magnetic surface are obtained. This experimental result encourages the attempt to reduce impurity content in a plasma by an axisymmetric divertor in a future large Tokamak. However, the plasma particle flux to the divertor region is not considered to be dominant part of the loss flux from the confined plasma in JFT-2a with the little dimensions and weak toroidal field. It is also shown that electric field is important to the plasma behavior near the separatrix magnetic surface.

By using four fast acting gas valves, the greater part of admitting gas are ionized and confined about 2 ms after the admission and it is shown that the particle influx to a plasma from thermal desorption is not dominant in the device. The typical plasma parameters are summarized below.

Plasma current	I_p = 20 kA
Divertor hoop current	$I_D = 0.9 \times I_p$
Pulse length	T_D = 30 ms
Mean electron density in the shell	$\bar{n}_{es} = 1.2 \times 10^{13}$ cm^{-3}
Conductivity temperature (assuming $\bar{Z}$=2 and uniform distribution)	T_e = 100 eV

Further detailed measurements including laser scattering and neutral particle energy analysis are under preparation.

Further experiment is required to be done especially concerning the particle and heat flux to the divertor region with and without flushing titanium.

Acknowledgements

The authors wish to thank Drs. M. Tanaka, S. Kunieda and members of the Thermonuclear Fusion Laboratory for fruitful discussions and encouragement. We are particularly indebted to K. Takahashi for the measurement of 4 mm microwave interometer and to K. Kumagai for the measurement of X-ray radiation.

REFERENCE

1) Yoshikawa, M. et al., Fifth Conference on Plasma Physics and Controlled Nuclear Fusion Research (Tokyo, 1974) Paper CN-33/A1-2.

2) Yoshikawa, M., Shimomura, Y., Maeda, H., and Kitsunezaki, A., Sixth European Conference on Controlled Fusion and Plasma Physics (Moscow, 1973) 173.

3) Kitsunezaki, A., Maeda, H., Shimomura, Y. and Yoshikawa, M., Third International Symposium on Toroidal Plasma Confinement (Garching, 1973) Paper G-2.

4) Annual Report of JAERI Thermonuclear Fusion Laboratory (for period ending March 31, 1972) JAERI-M 5029 (1972) 54.

5) Annual Report of JAERI Thermonuclear Fusion Laboratory (covering the period April 1, 1972 - March 31, 1973) JAERI-M 5564 (1974) 50.

6) Annual Report of JAERI Thermonuclear Fusion Laboratory (covering the period April 1, 1973 - March 31, 1974) JAERI-M 5888 (1974) 23.

7) Grelot, P. and Weisse, J., Sixth European Conference on Controlled Fusion and Plasma Physics (Moscow, 1973) 79.

8) Kitsunezaki, A., Maeda, H. and Shimomura, Y., Nuclear Fusion 14 (1974) 747.

9) Kitsunezaki, A., Shimomura, Y., Maeda, H. and Yoshikawa, M., JAERI-M 5612 (1974) (in Japanese).

10) Funahashi, A. et al., to be published JAERI-M (1975) (in Japanese).

11) To be published.

12) To be published.

13) To be published.